Geomorphology of the southernmost Longitudinal Valley fault: Implications for evolution of the active suture of eastern Taiwan

J. Bruce H. Shyu[1,*], Kerry Sieh[1], Yue-Gau Chen[2], Ray Y. Chuang[2,3], Yu Wang[1,2], and Ling-Ho Chung[2]

1: Tectonics Observatory, Division of Geological and Planetary Sciences, California Institute of Technology, Pasadena, CA 91125, USA

2: Department of Geosciences, National Taiwan University, Taipei, 106, Taiwan

3: Department of Geological Sciences, Central Washington University, Ellensburg, WA 98926, USA

* corresponding author; present address: Department für Geo- und Umweltwissenschaften, Ludwig-Maximilians-Universität München, Luisenstraße 37, 80333 München, Germany; Phone: +49-89-2180-6512. Fax: +49-89-2180-6514. E-mail: jbhs@gps.caltech.edu

Revised version submitted to *Tectonics* on 2007/04/26

Abstract

In order to understand fully the deformational patterns of the Longitudinal Valley fault system, a major structure along the eastern suture of Taiwan, we mapped geomorphic features near the southern end of the Longitudinal Valley, where many well-developed fluvial landforms record deformation along multiple strands of the fault. Our analysis shows that the Longitudinal Valley fault there comprises two major strands. The Luyeh strand, on the west, has predominantly reverse motion. The Peinan strand, on the east, has a significant left-lateral component. Between the two strands, late Quaternary fluvial sediments and surfaces exhibit progressive deformation. The Luyeh strand dies out to the north, where it steps to the east and joins the Peinan strand to become the main strand of the reverse sinistral Longitudinal Valley fault. To the south, the Luyeh strand becomes an E-W striking monocline. This suggests that the reverse motion on the Longitudinal Valley system decreases drastically at that point. The Longitudinal Valley fault system is therefore likely to terminate abruptly there and does not seem to connect to any existing structure further to the south. This abrupt structural change suggests that the development of the Longitudinal Valley suture occurs through discrete structural "jumps," rather than by a continuous northward maturation.

Keywords: Taiwan, tectonic geomorphology, Longitudinal Valley fault, river terraces, sutures.

Introduction

The island of Taiwan is the product of the ongoing collision of the Eurasian and the Philippine Sea plates [e.g., *Ho*, 1986; *Teng*, 1987, 1990; *Shyu et al.*, 2005a; and references therein] (Figure 1). As one of the very few places on Earth that is undergoing active suturing of lithospheric blocks, Taiwan provides valuable opportunities for understanding suturing processes. The collision involves three lithospheric blocks, separated by two sutures on the island [*Shyu et al.*, 2005a]. The eastern one, along the Longitudinal Valley in eastern Taiwan, is the active suture between the Luzon volcanic arc and a continental sliver that includes the Central Range, the mountainous backbone of Taiwan. The valley is very active seismically and contains many active structures, the most important being the Longitudinal Valley fault, one of the most active structures in the world [e.g., *Angelier et al.*, 1997; *Shyu et al.*, 2005b].

As the suturing matures from south to north, active structures of the Taiwan orogen manifest different characteristics, separating the island into several discrete neotectonic domains [*Shyu et al.*, 2005b] (Figure 2). Along the Longitudinal Valley are two: the Hualien and the Taitung Domains. In the Hualien Domain, which includes the northern third of the Longitudinal Valley fault, the fault appears to be predominantly sinistral and to slip at a lower rate. In the Taitung Domain to the south, the fault slips obliquely at a much higher rate, in association with the rapid uplift of the Coastal Range, in the hanging-wall block of the fault [*Yu and Liu*, 1989; *Hsu et al.*, 2003; *Shyu et al.*, 2006a].

Although the activity of the Longitudinal Valley fault has been known for decades and attracted numerous geodetic and seismologic investigations [e.g., *Angelier et al.*, 1997; *Lee et al.*, 2001, 2003; *Yu and Kuo*, 2001; *Kuochen et al.*, 2004; *Wu et al.*, 2006], there have been very few detailed geomorphic analyses of the fault. Most maps of the fault are large-scaled maps of the entire Longitudinal Valley, which contain very little detail [e.g., *Wang and Chen*, 1993; *Lin et al.*, 2000]. As a result, current knowledge of the fault is limited mostly to the main fault trace, which may absorb only a portion of the total deformation across the entire fault system. Without knowledge of details of the surface manifestation of the fault system, it is difficult to design proper experiments to observe the details of active deformation. For example, many of the current short-aperture geodetic experiments focus only on the main fault trace [e.g., *Lee et al.*, 2001, 2003], and may underestimate the slip rate of the fault.

Near the southern end of the Longitudinal Valley, a suite of well-developed fluvial surfaces provide a useful tool for mapping the Longitudinal Valley fault system in detail [*Shih et al.*, 1983, 1984]. The clear deformational patterns of these fluvial surfaces allow us to understand the characteristics of each strand of the fault. We have systematically mapped these geomorphic features to enable better interpretation of geodetic and seismologic data related to the kinematics of the fault.

A detailed understanding of the geometry of the southernmost section of the Longitudinal Valley fault system is also relevant to understanding the evolution of the suture. How does the suture first appear at its southern end? What is the relationship between the Longitudinal Valley fault and the subaqueous structures that border the colliding but as yet unsutured volcanic arc and the continental sliver to the south? Answers to these questions will enhance our knowledge of general suturing processes at arc-arc and arc-continent collisions.

Our principal means for geomorphic analysis is a set of digital elevation models (DEM), with 40-m resolution. Although a more recent 5-m resolution DEM covers only part of our study area, it significantly improved our ability to identify small features and secondary structures of the fault. In this paper, we present the combined results of our mapping using these two sets of DEM. Our DEM analysis was followed by mapping and investigations of fluvial landforms in the field.

Tectonic setting

Taiwan is forming at the boundary between the Philippine Sea plate and the South China block of the Eurasian plate (Figure 1). South of Taiwan, the oceanic South China Sea plate is subducting eastward beneath the Philippine Sea plate along the Manila trench. Above that subduction zone is the Luzon volcanic arc. At the latitude of Taiwan, however, the oceanic lithosphere of the South China Sea has been consumed entirely, and the Chinese continental margin has begun to impinge upon the trench, which results in the collision that is creating the mountainous island of Taiwan.

Although the Taiwan orogen has traditionally been viewed by most as a classic example of active arc-continent collision between the Luzon arc and the Eurasian continental margin [e.g., *Suppe*, 1987; *Teng*, 1990; *Huang et al.*, 1997; *Malavieille et al.*, 2002; and references therein], we have proposed an alternative model recently [*Shyu et al.*, 2005a]. The traditional views consider that the submarine Hengchun Ridge south of Taiwan is the accretionary wedge at the leading edge of the Manila trench, and the Central backbone Range of Taiwan, which is structurally continuous with the Hengchun Ridge, is composed by metamorphosed accretionary wedge sediments that were exhumed due to the collision (Figures 1 and 2). However, the presence of pre-Cenozoic continental basement in the Central Range of Taiwan [e.g., *Ho*, 1988] suggests that this strip may not be just a simple accretionary prism. Instead, we believe that it is a continental sliver that intervenes between the continental margin and the volcanic arc. Therefore, the orogen is formed by a tandem suturing between the Eurasian continental margin, the continental sliver, and the Luzon volcanic arc. In eastern Taiwan, the Longitudinal Valley suture is the suture between the docking volcanic arc of the Coastal Range and the Central Range, the metamorphic core of the continental sliver.

The east-dipping Longitudinal Valley fault is the major structure along this suture (Figure 2). Along the fault, the highly shortened volcanic rocks and forearc and intraarc basin sediments of the Coastal Range are thrusting over the current sediments of the

Longitudinal Valley. Slip rate along the fault is up to several tens of mm/yr [*Angelier et al.*, 1997; *Shyu et al.*, 2006a], making it one of the fastest slipping faults in the world. Ages of uplifted fluvial terraces in the Coastal Range near Rueisuei (Figure 2) suggest that the fault has been slipping at such high rates throughout at least the Holocene [*Shyu et al.*, 2006a]. Farther south along the fault near Chihshang, many small to moderate earthquakes illuminate the subsurface listric shape of the fault plane [*Chen and Rau*, 2002; *Kuochen et al.*, 2004].

On the western side of the Longitudinal Valley, the west-dipping Central Range fault slips at a lower rate than the Longitudinal Valley fault and is active along the southern two-thirds of the valley [*Shyu et al.*, 2006b] (Figure 2). Although currently not slipping at a high rate, geomorphic evidence of the fault is clear and widespread along the western side of the valley.

Although volcanic arc rocks and associated turbidite deposits of the Coastal Range generally constitute the hanging-wall block of the Longitudinal Valley fault, in the southern part of the valley, the Lichi Formation crops out immediately to the east of the fault as a very distinct stratigraphic unit. This unit consists of various and abundant blocks, sometimes tens of kilometers in size, within highly sheared, chaotic sand and mud matrix [*Ho*, 1988]. The Lichi Formation is either highly shortened and sheared deep marine forearc or intraarc basin sediments [e.g., *Biq*, 1971; *Teng*, 1981; *Hsü*, 1988; *Huang et al.*, 1992; *Chang et al.*, 2001] or slump deposits associated with mass wasting of sediments on the steep slopes that bound these basins [e.g., *Page and Suppe*, 1981; *Barrier and Muller*, 1984; *Barrier and Angelier*, 1986].

Major geomorphic features of the southernmost Longitudinal Valley

Along most of its length, the floor of the Longitudinal Valley is a low-relief plain between the Central and Coast Ranges, formed by several trunk rivers and their tributaries. In the southernmost part of the Longitudinal Valley, however, several fluvial terraces, locally up to 300 m above the current valley floor, exist between the two ranges (Figure 3). These terraces are underlain by late Quaternary alluvial deposits, mostly gravels and sand. Distinct members of these fluvial landforms, from south to north, are the Peinanshan, the Kaotai and Pingting terraces.

The Peinanshan, south of the eastward flowing Luyeh River, is a N-S elongated hill that perches up to 300 m above the Longitudinal Valley floor (Figure 3). This feature is also known as "The Foot," due to its peculiar shape in map view. Lateritic soils overlie most of the western part of the Peinanshan. Judging from the dates of similar lateritic terraces in other parts of Taiwan [e.g., *Chen*, 1988], this implies that fluvial terraces atop the western Peinanshan formed at least a couple tens of thousand of years ago. Late Quaternary Peinanshan Conglomerate underlies the lateritic soils of the fluvial terraces. This stratigraphic unit consists mostly of rounded fluvial cobbles of metamorphic rocks from the Central Range, including schist and marble clasts [*Hsu*, 1956; *Teng and Wang*, 1981; *Barrier et al.*, 1982]. Volcanic and sandstone clasts, probably from the Coastal Range, are present locally. In the eastern part of the Peinanshan, the Peinanshan Conglomerate is indurated and dips steeply.

Between the Luyeh and Luliao Rivers are the Kaotai and several lower terraces. The highest of these are also capped by lateritic soils. This and the fact that the Kaotai terraces rest at elevations that are similar to elevations of the Peinanshan terraces suggest that the highest Kaotai and Peinanshan terraces are probably similar in age. The lateritic soils of the Kaotai terraces are also underlain by fluvial cobbles derived mostly from the Central Range, which implies a source and origin similar to that of the Peinanshan Conglomerate.

Farther north, and east of the Luliao River, the small Pingting terraces appear to be uplifted Peinan River bed (Figure 3). The terraces divide into two major groups, the higher eastern one sitting about 50 m above the current riverbed. Uplift of the Pingting terraces has caused the current Peinan River to narrow significantly where it flows around the terraces. The lower elevation of the Pingting terraces above the current river bed suggests that they are much younger than the Peinanshan and the Kaotai terraces. This is consistent with the fact that no lateritic soil covers them. Instead, they are capped only by a thin layer of fluvial gravels, locally up to 10 m thick. On both the northern and southern flanks of the terraces, the Lichi Formation crops out beneath the thin fluvial gravels.

Neotectonic geomorphology of the Kaotai and surrounding terraces

Although the topographic features on the Kaotai and surrounding terraces are not the most impressive in the area, their relationship to underlying structures is the most straightforward, and provides a basis for understanding neotectonic geomorphic features elsewhere in the area. North of the Luyeh River, geomorphic features clearly indicate that a major reverse fault cuts across large river terrace 4, on which the village of Lungtien sits (Figure 4). This reverse fault extends further to the north and forms the approximate boundary of the Kaotai terraces and the Central Range. Still further to the north, the fault appears to die out to the north, just shy of the Luliao River.

A very clear monoclinal scarp, up to 15 m high, runs N-S across the Lungtien terrace north of the Luyeh River, just west of Lungtien (Figures 4 and 5a). Between Lungtien and the scarp, the surface of the terrace forms an anticlinal warp. Other than the scarp and the warp, the Lungtien terrace surface shows a gentle eastward slope that is consistent with its Luyeh River origin. Therefore, we believe the scarp and the anticline are manifestations of a fault-propagation fold up-dip of an east-dipping blind reverse fault beneath the eastern part of the Lungtien terrace. In fact, this clear feature was identified as an active structure long ago, and was named the Luyeh fault by several investigators

[*Shih et al.*, 1983, 1984, 1986; *Yang*, 1986; *Chu and Yu*, 1997]. It has been considered generally to be a thrust strand of the Longitudinal Valley fault. Since this reverse fault is a strand of the Longitudinal Valley fault, we refer to it as the Luyeh strand.

From a shallow pit dug into the terrace surface east of Yenping, we collected a charcoal sample from the gravel beds that underlie the Lungtien terrace. The sample yielded a calibrated age of about 3.35 ka (Figure 4; Table 1), which represents a maximum age for the terrace surface. Since the terrace surface has been offset vertically about 15 m by the Luyeh strand (Figure 5a), the minimum vertical slip rate of the strand is about 4.5 mm/yr. Because the gravel beds containing the charcoal sample are close to the terrace surface, we believe that the age of the sample is close to the age of the terrace surface, and the 4.5 mm/yr minimum is close to the true vertical slip rate of the Luyeh strand.

On the southern edge of the Lungtien terrace, the Luyeh strand descends a small south-flowing canyon toward the active bed of the Luyeh River, which divides terrace 3 into two patches (Figure 4). Terrace 3, which is about 10 m lower than terrace 4, has been clearly offset by the Luyeh strand, since the small patch of terrace 3 east of the canyon is about 10 m higher than its counterpart west of the canyon (Figure 5b). Younger terrace 1, however, does not display an offset by the Luyeh strand. If terrace 1 predates the most recent displacements, the magnitude of the offset is too small to be seen in the cultivated surface of the terrace.

North of the Lungtien terrace, the Luyeh strand extends into the valley between the Kaotai terraces and the Central Range (Figure 4). The Kaotai terraces cap a large, broad anticline, shown both by sloping terrace surfaces and bedding attitudes in the underlying gravels beds. This anticline may be the northern extension of the small anticline west of Lungtien and may also be a fault-propagation fold up-dip of the Luyeh strand.

West of the Kaotai terraces, the Luyeh strand branches into three discrete sub-strands (Figure 4). At least one of these sub-strands, along the western front of the terraces, appears to break the surface as a reverse fault. The westernmost strand, however, appears as a monocline. This monoclinal strand has produced a series of anticlinal ridges of colluvium in the valley between the Kaotai terraces and the Central Range and cuts through an E-W striking ridge of metamorphic slates of the Central Range (point S in Figure 4). Therefore, although most of the deformation caused by the Luyeh strand concentrates in late Quaternary gravels underlying the Kaotai terraces, the westernmost sub-strand has involved a small piece of the Central Range. This may be the only place where part of the Longitudinal Valley fault system extends so far to the west that it deforms the Central Range.

On the highest surface of the Kaotai terraces (terrace 7) are several gentle E-W striking scarps (Figure 4). These scarps most likely are minor normal fault scarps formed athwart the anticlinal axis parallel to the convergence direction, analogous to those found in southern Tibet [e.g., *Molnar and Tapponnier*, 1978; *Yin et al.*, 1999; *Blisniuk et al.*, 2001]. Alternatively, these gentle scarps may reflect irregularities in the geometry of the underlying fault, caused by its overriding of an irregular surface on the footwall block.

Since the minimum vertical slip component of the Luyeh strand is about 4.5 mm/yr, we can estimate the minimum age of the highest Kaotai terraces. Assuming that the floor of the canyon between the Kaotai terraces and the Central Range is correlative with the highest surface (terrace 7) above the Kaotai terraces, the surface has been uplifted at least 135 m. This yields and age of at least 30 kyr for the Kaotai terrace 7, consistent with their being capped by lateritic soils.

Kaotai terrace 7 ends abruptly at an E-W trending drainage just south of the village of Yungan (Figure 4). However, the Luyeh strand continues northeastward as a series of anticlinal ridges on lower terraces. The height of these ridges decreases to the north. The fact that relief on the folds decreases northeastward on the same terraces indicates the folds die out to the northeast. The northernmost and lowest anticlinal ridge ends just south of terrace 2 of the Luliao River. No deformation is visible on the low terraces 1 and 2 of the Luliao River farther northeast.

Deformation of the Luanshan Bridge (LSB in Figure 4), which crosses the Peinan River southeast of Luyeh, indicates that another strand of the Longitudinal Valley fault east of the Luyeh strand, within the Peinan River valley. We refer to this strand as the Peinan strand. About 200 m from the eastern end of the Luanshan Bridge, the bridge roadbed has been fractured by east-west compression (Figure 6a). Since the bridge was last repaired in early 2003, the damage may well have resulted from minor slip of the Peinan strand during the December 2003 Mw 6.8 earthquake [*Wu et al.*, 2006; H.-T. Chu, personal communication, 2004]. Because fractures of the bridge roadbed appear only at this point, and the bridge consists, ostensibly, of identical sections, the Peinan strand likely crosses beneath the bridge section that contains this fracture, about 200 m from the eastern abutment (Figure 4).

Although topographic features of the Peinan strand are rare, the existence of this strand is suspected on the basis of geodetic observations across the Peinan River farther south, near Taitung. Measurements there show that the two sides of the river have left-lateral movement relative to each other [e.g., *Yu et al.*, 1992]. This pattern led many to believe that this is a typical slip-partitioning of the Longitudinal Valley fault, with a reverse Luyeh strand and a sinistral Peinan strand [*Lee et al.*, 1998; *Hu et al.*, 2001]. However, it may not be this simple. The deformation of the Luanshan Bridge indicates that the Peinan strand has significant reverse motion. Moreover, the vertical slip component of the Luyeh strand, at about 4.5 mm/yr, is much less than the vertical slip component of the Longitudinal Valley fault observed along its other segments, which may be more than 20 mm/yr locally [*Yu and Liu*, 1989; *Angelier et al.*, 1997; *Lee et al.*, 2001, 2003; *Shyu et al.*, 2006a]. Therefore, we believe that although the Longitudinal Valley fault branches into two strands, at least between the Luyeh and Luliao Rivers its slip is not completely separated into strike-slip and dip-slip components.

Neotectonic geomorphology of the northern Peinanshan area

South of the Luyeh River, the Luyeh strand extends along the western edge of the Peinanshan and underlies a large anticline-syncline pair, as shown by the deformed highest terrace surface on the Peinanshan (Figure 7). The Peinan strand appears to become more sinistral and cuts the northeastern corner of the Peinanshan.

Geomorphic features indicate that the surface trace of the Luyeh strand extends southward along the western edge of the Peinanshan (Figures 7 and 8). Narrow scarps east of the village of Chulu, for example, suggest that the fault breaks the surface. Slip on the Luyeh strand has juxtaposed the northwestern corner of the Peinanshan against a ridge of metamorphic rocks of the Central Range. Since the bedrock ridge shows no geomorphic evidence of deformation, we believe the Luyeh strand must crop out in the small canyon flowing northward between the ridge and the Peinanshan. If so, this part of the Luyeh strand has not yet faulted any of the Central Range rocks.

In the hanging-wall block of the Luyeh strand is an anticline-syncline pair (Figure 7). These folds are clearly manifest in the deformed surface of terrace 7 on the northern Peinanshan (Figure 8a) and in bedding attitudes of the underlying gravel beds. On the younger terraces along the northern side of the Peinanshan, the two folds have smaller amplitudes than they do on the older terrace 7 (Figure 8b). Moreover, the bedrock gravels dip more steeply than the terrace 7 surface. These features indicate that the folds have been growing progressively during deposition of the gravels and subsequent incision of the Luyeh River.

South of Chulu, the two folds turn slightly to the southwest and are truncated by the Luyeh strand (Figure 7). Horizontal gravel beds along the small southwestward-flowing canyon south of Chulu suggest that the synclinal axis may follow the canyon and connect with the Luyeh strand further south.

We are not sure if the anticlinal axis extends further north under the Luyeh River and connects with the anticlines west of Lungtien or beneath the Kaotai terraces. The synclinal axis, however, does appear to extend to the north and turns northeastward (Figures 4 and 7).

East of the synclinal axis, the dip of the Peinanshan Conglomerate steepens to the east, becoming vertical near the eastern edge of the Peinanshan (Figure 7). This is evident from the presence of clear bedding plane ridges near the northeastern corner of the Peinanshan, and by the bedding attitude measurements along the eastward flowing canyon south of the village of Shanli. The presence of very steep beds in the eastern limb of the syncline and the fact that the synclinal axis merges to the south with the Luyeh strand suggest that the syncline formed as a fault-propagation fold. The gentle limbs of the anticline, on the other hand, suggest that the anticline is a fault-bend fold. Therefore, the two folds found in the northern Peinanshan may represent structures developed in different stages. The syncline may have developed first, as a fault-propagation fold up-dip of a blind Luyeh strand. Later, when the tip of Luyeh strand broke the ground surface, a bend formed along the fault plane as the hanging wall rode over the ground surface and produced the gentle anticline. The Luyeh strand along the southern part of the Peinanshan breaks the surface along the synclinal axis, but no anticline has developed. More detailed subsurface information, such as seismic reflection profiles across different parts of the Peinanshan, is needed to verify our structural hypotheses.

On the surface of terrace 7 are many NNW-striking scarps (Figure 7). The origin of these scarps is controversial. Some believe that they are terrace risers formed by eastward migration of the Luyeh River during the uplift of the Peinanshan [*Shih et al.*, 1986; *Yang*, 1986]; others suggest that they represent active fault scarps [*Shih et al.*, 1983, 1984]. The presence of several west-facing scarps argues against an origin as terrace risers. Furthermore, at least along the westernmost scarps, the paleo-current direction in gravel outcrops is perpendicular to the scarps. Therefore, we favor a fault scarp origin. Due to the steepness of the scarps and the horst-and-graben-like topography, we suspect that they are normal faults. Their limited distribution and their strike direction suggest that they formed due to the indentation of the metamorphic rock ridge of the Central Range into the northwestern corner of the Peinanshan.

The Peinan strand cuts through the northeastern corner of the Peinanshan (Figures 7 and 8). South of the confluence of the Luyeh and Peinan Rivers, a ~5 m high, east-facing scarp cuts terrace 1. The scarp appears to extend to the south into the hills and to connect with another scarp on terrace 2 just northeast of Shanli. In fact, the latter scarp has been identified previously as the Shanli fault [*Shih et al.*, 1983, 1984, 1986; *Yang*, 1986]. In contrast to the scarp south of the Luyeh River, the Shanli scarp is higher and faces west. Because of this scissoring, we suspect that the Peinan strand south of the Luyeh River is predominantly a strike-slip fault.

On the eastern side of the Peinan River, across from the Luyeh River junction, an enormous landslide complex has formed on the western flank of the Coastal Range (Figure 7). The headscarps of this landslide complex are close to the crest of the Coastal Range, and the toes rest upon thin fluvial gravels on a bedrock strath, about 80 m above the current Peinan River bed (Figure 9a). The thickness of this landslide deposit locally exceeds 100 m. Since wood fragments found in the landslide deposits yielded ages that range from less than 1 ka to more than 2 ka (Figure 7; Table 1), the landslide deposits may have a complex history of multiple mass-wasting events.

The presence of a thin layer of rounded fluvial gravels between the bedrock strath and the landslide deposit (Figure 9b) indicates that the landslide toe rode out over either the active channel or an uplifted terrace of the Peinan River. In fluvial gravels above the terrace 2 strath just east of Luanshan Bridge, we found a charcoal sample about 18 m above the current Peinan River bed that yielded a calibrated radiocarbon age of about 1.1ka (Figure 4; Table 1). This yields an incision rate of about 16.4 mm/yr for the

Peinan River. If this incision rate of the Peinan River has been constant throughout the 80 m of uplift of the strath overridden by the landslide toe, the age of the toe is about 4.9 ka.

On some previous maps, the contact between the Lichi Formation and the Peinanshan Conglomerate appears as the major fault plane of the Longitudinal Valley fault [e.g., *Wang and Chen*, 1993]. An outcrop of this highly sheared contact is present on the eastern Peinan River wall across the junction of the Luyeh River (Figures 7 and 9a). The same contact appears in a small canyon farther north (Figure 9c). Although this highly sheared contact clearly is a major fault plane, it does not offset of the landslide deposits or underlying strath. Hence, it must have ceased activity sometime before the emplacement of the landslide toe. Further to the south, however, at the northeastern corner of the Peinanshan, the Peinan strand is active where it cuts through a hill and separates a large limestone block of the Lichi Formation on the east from Peinanshan Conglomerate on the west.

It is interesting that the old contact, covered by the landslide deposits, is located in the middle of an old Peinan River bed, very similar to the current situation, where most of the Peinan strand locates within the present Peinan River bed. Therefore, we suspect that the covered Lichi-Peinanshan contact may have been the active Longitudinal Valley fault strand right before the landslide occurred. Reverse faults are known to be sensitive to overlying topography and break into new branches if there is a significant overburden. For example, during the 1971 San Fernando earthquake in southern California, the fault at one location ruptured to the toe of a new man-made cut slope, rather than along its previous trace (e.g., Oakeshott, 1975). The additional load of the landslide deposits may thus cause the strand to propagate a new trace further west to find the river valley after the landslide. If this is the case, the current Peinan strand near the confluence of the Luyeh and Peinan Rivers would be a young feature, probably just a couple of thousand years old. This would be consistent with the obscure topographic features of the strand there.

Neotectonic geomorphology of the southern Peinanshan area

The southern Peinanshan area is the southernmost point of the Longitudinal Valley, and structures there should reflect the initial characteristics of the Longitudinal Valley suture. Slip on the Luyeh strand, in fact, decreases southward from the central Peinanshan and ceases altogether at the southern tip of the Peinanshan. This indicates that the majority of the Longitudinal Valley fault system ends at the southern tip of the Peinanshan, and does not connect to structures farther south.

Several observations point to the southward decrease of the slip on the Luyeh strand. Along the western front of the southern Peinanshan, the Luyeh strand appears to break the ground surface, locally producing fault scarps on young alluvial surfaces (Figure 10). By contrast, the southernmost part of the Luyeh strand wraps eastward around the southern Peinanshan and turns into an E-W striking monocline, evidenced by a series of southward tilted terraces. Moreover, the elevation of the terrace 7 surface, on the hanging-wall block of the Luyeh strand, also decreases southward. Together, these observations imply that slip on the fault decreases significantly southward.

The E-W striking monocline at the southern tip of the Peinanshan marks the last appearance of the Luyeh strand. In the southern Peinanshan, several secondary monoclines, generally with steeper eastern surfaces and gentler western surfaces, deform the terrace 7 surface (Figure 10). One of the monoclines extends along the large N-S trending canyon there and replaces the fault as the major structure of the southernmost Luyeh strand. At the southernmost part of the Peinanshan, several southwestward tilting surfaces of terrace 7 are present. The bedding attitudes of the gravel beds underlying the easternmost one are very similar to the slope of the surface itself. Thus, it is clear that slip on the Luyeh strand is dying out and becomes zero immediately south of the monocline.

Progressive tilting of terraces 2 and 3 further to the east supports this interpretation. Both terraces are strath terraces, since only a thin layer of fluvial beds deposited on Peinanshan Conglomerate underlie them near the village of Yenwan. Thus, the slope of the terrace surfaces was not produced by deposition. The fact that terrace 3 is steeper than terrace 2 and that terrace 2 is steeper than the active floodplain implies progressive southward tilt. This progressive tilt of the terraces supports the conclusion that the Luyeh strand dies out at the southern tip of the Peinanshan, last appearing as an E-W striking monocline.

West of the small village of Pinglang, a N-S trending anticlinal ridge with a monoclinal western front disturbs alluvial surfaces (Figure 10). The ridge has a maximum height of about 10 m and dies out gradually to the south on the active Taiping River fan. This geomorphic expression is the only information available for this minor structure, but it suggests that this feature represents a young east-dipping thrust fault that is subsidiary to the Luyeh strand.

The location of the Peinan strand is ambiguous along most of its course east of the southern Peinanshan. Its only geomorphic expression east of the southern Peinanshan is near the village of Lichi. North of Lichi, a small N-S striking scarp separates terraces 2 and 3 (Figure 10). Although this scarp may be just a fluvial terrace riser, the fact that it is also coincident with the contact between the Lichi Formation and the Peinanshan Conglomerate suggests it may be a fault scarp. Since the mud-rich Lichi Formation (on the east) is much more erodable than the Peinanshan Conglomerate, a west-facing scarp there supports the notion that it is a fault scarp rather than an erosional terrace riser.

Farther south, the location of the Peinan strand is very ambiguous, but deformation of two bridges across the Peinan River may help locate the fault trace. Close to the eastern end of the Lichi Bridge (LCB in Figure 10), the bridge appears to be slightly deformed (Figure 6b), but the deformation may be simply due to poor construction.

Further to the south, geodetically measured left-lateral creep of about 25 mm/yr near the Taitung Bridge [*Yu et al.*, 1992] (TTB in Figure 10) indicates that the Peinan strand runs very close to the bridge.

Neotectonic geomorphology of the Pingting terraces

In previous sections, we have described from north to south the two major strands of the Longitudinal Valley fault (Figures 4, 7 and 10). Farther north, the fault does not partition into two widely separated, distinct strands. In the northwestern corner of Figure 3 and in the vicinity of the Luliao River, the Longitudinal Valley fault has clear expression only at the Pingting terraces. Since the Luyeh strand does not continue north of the Luliao River, all slip on the Longitudinal Valley fault seems to be concentrated on strands at the Pingting terraces, near the eastern edge of the valley.

The Pingting terraces consist of two major steps, each bounded by a N-S trending and west-facing scarp (Figure 11). Both steps consist of several different terraces. The large abandoned alluvial fan of Luliao River abuts the western scarp.

Although the two N-S trending scarps bounding the two Pingting steps may simply be fluvial terrace risers, we believe that they are the two principal oblique-slip strands of the Longitudinal Valley fault and that the Pingting terraces are old Peinan River beds that have been uplifted along the two strands. Two lines of evidence support this hypothesis: First, the Pingting terraces are strath terraces and the Lichi Formation underlies the thin fluvial gravels beneath the terrace surfaces. Thus the Pingting terraces are east of and on the hanging-wall block of the Longitudinal Valley fault system. Second, the current Peinan River flows east of the Pingting terraces farther into the hanging-wall block of the Longitudinal Valley fault (Figure 11). If the two west-facing scarps were simply terrace risers formed as the Peinan River cut into the western portion of the Pingting terraces, it would be hard to explain how the Peinan River could later abandon these channels and develop a new channel in the rapidly uplifting hanging wall of the Longitudinal Valley fault. The scarps are difficult to attribute to erosion of the Luliao River as well, since the scarps are perpendicular to its flow direction.

An outcrop on the southern side of the Pingting terraces shows that the eastern scarp is indeed a fault scarp (point R in Figure 11). In this man-made excavation, the Lichi Formation clearly thrusts over fluvial gravels along a fault that dips about 70° to the east. The slightly warped surfaces of the eastern Pingting step likely reflect an anticlinal warp on the hanging-wall block of this fault. South of point R, the terrace risers of terrace 2 have been clearly offset left-laterally about 15 m by this fault. Terrace 2 is also about 10 m higher in the hanging wall of the fault than in the footwall. Therefore, this fault clearly has both reverse and sinistral motions. Left-lateral offset by this fault is also clear across the riser between terraces 1 and 2 near the northern end of the Pingting terraces.

Characteristics of the western Pingting scarp are less well constrained. Although this strand may also have sinistral component, there is no good geomorphic evidence. Just southwest of the Pingting terraces, the fault exhibits a series of *en echelon* minor strands that step slightly to the west and connect with the Peinan strand (Figure 11). These scarps on terrace 2 are all less than 5 m high.

Since both of the west-facing Pingting scarps are strands of the Longitudinal Valley fault, we believe that the highest terrace surface on each of the Pingting steps may be correlated with the surface of the abandoned Luliao River fan. The lower and minor terraces on each Pingting step may have been cut by smaller channels during the abandonment of the terraces. Southeast-directed paleo-currents in a gravel bed beneath a slightly lower triangular surface on the higher eastern Pingting step (at point F in Figure 11) support this hypothesis. The small terrace was probably formed by a small stream that flowed southeastward across the rising Pingting terraces into the Peinan River. The narrowest part of this terrace is coincident with the anticlinal axis, which is consistent with the hypothesis that the terrace formed while the anticline is growing, and the growth of the anticline outpaced the incision of the minor channel.

If the highest terrace surface on each of the Pingting steps is correlative, we may calculate the uplift rate using the age of the terraces. A charcoal sample from an outcrop of gravel beds about 2 m beneath the western Pingting terrace yields a calibrated radiocarbon age of about 1.6 ka (Figure 11; Table 1). If the highest terrace 6 on the eastern Pingting step has the same age, the elevation difference of about 25 m between the two Pingting steps yields an uplift rate by the eastern strand of about 15.6 mm/yr. Furthermore, if the abandoned Luliao River fan west of the Pingting terraces also has a similar age, the uplift rate by the western strand would be about 12.5 mm/yr, based upon the about 20 m uplift of the western Pingting step. Assuming there is no other major strand of the Longitudinal Valley fault in the vicinity of the Pingting terraces, the minimum total vertical slip component of the fault would be about 28 mm/yr. If we consider the observed 70° eastward dip of the fault to be representative, the minimum slip rate along the fault would be about 30 mm/yr.

The location of the Longitudinal Valley fault north of the Pingting terraces is not well constrained, but deformation of the Paohua Bridge (PHB in Figure 3), about 3 km to the north, indicates that the fault is in the Peinan River bed (Figure 11). The bridge was clearly deformed by fault rupture during the December 2003 earthquake about 100 m from its eastern abutment [H.-T. Chu, unpublished data, 2004] (Figure 6c).

Discussion

"The Foot," the valley, and the mountains: Implications for the development of the Longitudinal Valley suture and the Taiwan orogen

The southern end of the Taitung Domain: structural development between domains

As the active suturing that is producing the island of Taiwan matures from south to north, active structures of the island show different characteristics. This led us to propose that the Taiwan orogen consists of several discrete neotectonic domains [*Shyu et al.*, 2005b]. In eastern Taiwan from south to north are the Lutao-Lanyu, Taitung, Hualien, and Ryukyu Domains. Each domain is defined by a distinct suite of active structures, and from one domain to the next the major structures behave differently. This significant change in behavior sometimes occurs through a transition zone, where characteristics of both neighboring domains are superimposed. Since the Peinanshan area is at the southern end of the Taitung Domain (Figure 2), the structures there should reflect the structural characteristics of the boundary between the Taitung Domain and the Lutao-Lanyu Domain to the south.

Our geomorphic analysis of the southern Peinanshan indicates that the magnitude of reverse motion on the Luyeh strand decreases significantly southward. The elevation of terrace 7 decreases southward and the southernmost expression of the Luyeh strand is as a monocline that wraps around the southern Peinanshan. Although the Peinan strand, with its sinistral motion, may extend further to the south, the reverse motion on the Luyeh strand clearly dies out at the monocline. This coincides with the dramatic decline and disappearance of the Coastal Range to the east.

We propose that the coincident southern termini of the Luyeh strand, the Peinanshan and the Coastal Range represent the southern termination of the Taitung Domain. To the south, the major structure in the Lutao-Lanyu Domain is a west-dipping thrust fault beneath forearc basin sediments, and no east-dipping structure equivalent to the Longitudinal Valley fault is present [*Shyu et al.*, 2005b] (Figure 2). The west-dipping thrust fault does not connect to any structure in the Taitung Domain and appears to end south of Taitung. The structural characteristics of the southern end of the Taitung Domain are therefore consistent with our hypothesis that significant changes of structural behavior occur across the boundaries of the neotectonic domains of Taiwan.

The development of the Longitudinal Valley suture

Since the southern end of the Taitung Domain is where the Longitudinal Valley suture of eastern Taiwan starts to appear, structural characteristics there have significant implications for the development of the suture. Recently, when we attempted to estimate the Holocene slip rate of the Longitudinal Valley fault from uplifted fluvial terraces, we found that although the fault appears to be more or less continuous in map view, the subsurface geometry of the fault varies significantly [*Shyu et al.*, 2006a]. The fault extends to much greater crustal depths in its southern reaches than farther north, where we did our analysis. This new finding, combined with our analysis of the Central Range fault on the western side of the valley [*Shyu et al.*, 2006b], motivated us to propose a model for the development of the Longitudinal Valley suture (Figure 13). In this model, the sequential development of multi-tiered reverse-fault wedges facilitates the thickening of the margins of both non-oceanic blocks across the Longitudinal Valley suture and results in the development of a "Christmas tree" shaped suture.

The structural characteristics of the southernmost Longitudinal Valley are also consistent with such a model. In the Lutao-Lanyu Domain, the west-dipping thrust fault beneath the forearc basin sediments represents the first generation of west-dipping reverse-fault wedges. Only at the latitude of Taitung, where the colliding Luzon arc gets close enough to the Central Range block, does the west-vergent Longitudinal Valley fault begin to appear. This is the second discrete jump in development of the Longitudinal Valley suture. This mode of formation of the suture contrasts with a continuous maturation of existing structures. These structural "jumps" involve structures at different structural levels on both sides of the suture. In addition, the multi-tiered reverse-faulting geometry requires accommodation structures to connect major reverse-fault wedges at different crustal depths. In the southernmost Taitung Domain, the E-W striking monocline may represent one such accommodation structure.

The development of the Taiwan orogenic belt

The island of Taiwan is produced by the ongoing collision between the Eurasian and the Philippine Sea plates. The Longitudinal Valley in eastern Taiwan, between the Coastal and the Central Ranges, has long been considered to be the locus of suturing in this collisional orogen. Therefore, the structural characteristics of the southernmost part of the valley have long been known to have important implications for the development of the orogenic belt.

One of the major puzzles of the Taiwan orogen is the composition of the Central Range, the mountainous backbone of the island. The traditional point of view is that the Central Range is merely an exhumed and uplifted accretionary wedge. However, the presence of pre-Cenozoic continental basement in the Central Range rocks [e.g., *Ho*, 1988] suggests that the range is a continental sliver sandwiched between the Eurasian continental margin and the Luzon volcanic arc [*Shyu et al.*, 2005a]. In our model, the slates and schists of the Central Range that overlie the continental basement are metamorphosed Eocene to Miocene continental margin sediments that were deposited upon and then rifted with the continental sliver.

The abrupt appearance of the Longitudinal Valley suture at the southern end of the Taitung Domain is consistent with this hypothesis. At the latitude of Taitung, the colliding Eurasian continental margin is still far to the west of the volcanic arc, on the west side of the Central Range (Figures 1 and 2). Therefore, the development of the Longitudinal Valley suture near the Peinanshan indicates that the Central Range is rigid crustal block between the continental margin and the volcanic arc. If the Central Range comprises only accretionary wedge sediments, convergence between the Eurasian continental margin and the volcanic arc would be expected within the range at the latitude of Taitung. The result would be numerous active structures across the range, and a narrower, discrete suture would only appear farther north, at a point where continental margin and volcanic arc crusts actually collide. Instead, a well-defined suture occurs in the southernmost Longitudinal Valley, with structures that are accommodating up to 30 mm/yr of reverse slip, and no major structures have been observed in the Central Range at the same latitude. The presence of the Central Range fault, which is blind near the Peinanshan but emergent farther north [*Shyu et al.*, 2006b], also implies that the range is acting as a rigid block.

In summary, the southernmost Longitudinal Valley is a small but critical area for understanding the Taiwan orogenic belt. The abrupt appearance of the Longitudinal Valley fault system there is consistent with the hypothesis that the orogen comprises several distinct neotectonic domains characterized by abrupt changes of structural behavior across domain boundaries [*Shyu et al.*, 2005b]. The Longitudinal Valley suture therefore appears to be forming through several discrete structural "jumps," rather than through a continuous maturation of existing structures. In cross-section these jumps appear as two opposing families of imbricated reverse faults, reminiscent of the geometry of a Christmas tree [*Shyu et al.*, 2006a, b]. Furthermore, the appearance of the suture at the latitude of Taitung is consistent with our hypothesis that the Central Range of Taiwan is a continental sliver sandwiched between the collision of the Eurasian continental margin and the Luzon volcanic arc [*Shyu et al.*, 2005a].

The Central Range fault in the southernmost Longitudinal Valley

All of the neotectonic features we have mapped in the Peinanshan area are components of the east-dipping Longitudinal Valley fault system. The west-dipping Central Range fault, though active and emergent in the middle part of the Longitudinal Valley, does not appear to break the ground surface in this area [*Shyu et al.*, 2006b] (Figure 2). Instead, the fluvial terraces along the northern bank of the Luyeh River provide evidence that the Central Range fault is active but blind.

West of and in the footwall block of the Luyeh strand, the Lungtien terrace (terrace 4) sits up to 60 m above the current Luyeh River bed (Figure 5a). The absence of any other strand of the Longitudinal Valley fault west of the Luyeh strand indicates that the incision of the Luyeh River to produce the Lungtien and other terraces west of the Luyeh strand is caused by uplift of the eastern flank of the Central Range. In fact, the surface break of the Lungtien terrace by the Luyeh strand appears to be just a small irregularity overprinted on the far greater incision of the Luyeh River. Therefore, we believe the overall uplift of the eastern flank of the Central Range and the Luyeh River terraces results from slip on a blind Central Range fault. The fault would have to be overridden by the Luyeh strand, which breaks the surface of the Lungtien terrace (Figure 12).

The Lungtien terrace is a fill terrace, underlain by thick fluvial deposits. At point N in Figure 4, a 40-m high outcrop consists entirely of young fluvial gravels beneath the Lungtien terrace surface. Thus the thickness of fluvial gravels underlying the Lungtien terrace is more than 40 m. This indicates that although the Luyeh River has cut about 60 m into the Lungtien terrace, the net bedrock uplift of the terrace west of the Luyeh strand is less than 20 m. Since the age of the Lungtien terrace is about 3.5 ka, the uplift rate of the eastern Central Range flank can be no more than 6 mm/yr. This is consistent with the suggested uplift rate of less than 6.4 mm/yr related to slip on the Central Range fault farther north [*Shyu et al.*, 2006b].

Surface creep of the southernmost Longitudinal Valley fault

It is well-known that the Longitudinal Valley fault is creeping aseismically at rates as high as 20 mm/yr near Chihshang, about 30 km north of the Peinanshan [*Angelier et al.*, 1997; *Lee et al.*, 2001, 2003] (Figure 2). Other segments of the fault, however, may be locked.

We conclude that the Luyeh strand of the fault is not creeping at the surface, because we found no place where any man-made structure is broken along the entire length of the fault. However, a leveling line installed in 2002 across the Luyeh strand scarp on the Lungtien terrace shows rapid deformation across an aperture of less than 3 km. This implies that although it is not creeping at the surface, the Luyeh strand is indeed creeping at a very shallow depth.

Although several bridges built across the Peinan strand are deformed, most of the deformation may have occurred during the December 2003 earthquake, by minor coseismic slip or aftercreep [H.-T. Chu, unpublished data, 2004]. Preliminary results of a short-aperture GPS transect across the Peinan strand at the northeastern corner of the Peinanshan show that no significant near-field velocity difference is present across the strand, which indicates that the strand may not be creeping at the surface at that point.

A short-aperture GPS transect across the Pingting terraces shows that large near-field velocity differences are present across the two strands of the Longitudinal Valley fault there. Since we did not find any broken man-made structures in this area, we believe that the strands may be similar to the Luyeh strand, in that they have a very shallow locking depth but are not creeping at the surface.

Conclusions

Fluvial landforms allow detailed mapping of the Longitudinal Valley fault system near its southern terminus in eastern Taiwan. The fault system branches into two major strands: the Luyeh strand in the west and the Peinan strand in the east. The Luyeh strand has predominantly reverse motion, whereas the Peinan strand has a significant sinistral component. Complete slip-partitioning, however, does not occur throughout this reach, because the Peinan strand may also have a large reverse component north of the Luyeh River.

The Luyeh strand produces a monoclinal scarp on the Lungtien terrace. Both to the north and to the south of the Lungtien terrace, old fluvial surfaces of the Kaotai terraces and the Peinanshan are moving upward and westward against the eastern flank of the Central Range. From the age of the Lungtien terrace, the minimum vertical slip component of the Luyeh strand is about 4.5 mm/yr. The Luyeh strand terminates to the south in an E-W striking monocline that wraps around the southern Peinanshan.

The Peinan strand appears to traverse the current Peinan River bed for most of the fault's length. The only exceptions are northeast of Shanli and on the terraces near Lichi, where the strand offsets fluvial terraces and produces small scarps. South of the Luyeh River, the Peinan strand is likely to be predominantly left-lateral.

The Luyeh strand steps to the east south of the Luliao River and joins with the Peinan strand to form the main strand of the Longitudinal Valley fault, which runs along the western edge of the Pingting terraces and extends to the north. The southern end of the Luyeh strand, on the other hand, is coincident with the southern end of the Coastal Range, and is likely to represent the abrupt southern termination of the Taitung Domain. Most of the active strands in the Peinanshan area have very shallow locking depths, but do not seem to be creeping at the surface.

The structural characteristics of the southernmost Longitudinal Valley suture suggest that the suture developed through several discrete structural "jumps," rather than through a continuous maturation of existing structures. These structural "jumps" involve imbricate structures on both sides of the suture.

Acknowledgments

We greatly appreciate the assistance of Y.-C. Chen and T. Watanuki in the field. We have benefited significantly from the information collected by and the stimulating discussions with the students of two bi-national field classes of the National Taiwan University and Caltech, held in the Peinanshan area in 2001 and 2005. We are also grateful for valuable discussions with H.-T. Chu, J.-C. Lee, W.-T. Liang, D.V. Wiltschko, Y.-M. Wu, and S.-B. Yu. Our mapping was facilitated by J. Giberson, manager of the Caltech's GIS laboratory. The 5-m DEM was generously provided by the Central Geological Survey, MOEA, Taiwan. Radiocarbon dating by M. Kashgarian in the Center for Accelerator Mass Spectrometry, Lawrence Livermore National Laboratory, is greatly appreciated. The comments and suggestions of E. Kirby and two anonymous reviewers greatly helped us improve this manuscript. Our project in Taiwan was supported by NSF grant EAR-0208505 and by the Gordon and Betty Moore Foundation. This is Caltech Tectonics Observatory Contribution #28.

References

Angelier, J., H.-T. Chu, and J.-C. Lee (1997), Shear concentration in a collision zone: kinematics of the Chihshang Fault as revealed by outcrop-scale quantification of active faulting, Longitudinal Valley, eastern Taiwan, *Tectonophysics*, *274*, 117-143.

Barrier, E., and J. Angelier (1986), Active collision in eastern Taiwan: the Coastal Range, *Mem. Geol. Soc. China*, *7*, 135-159.

Barrier, E., and C. Muller (1984), New observations and discussion on the origin and age of the Lichi Mélange, *Mem. Geol. Soc. China*, *6*, 303-325.

Barrier, E., J. Angelier, H. T. Chu, and L. S. Teng (1982), Tectonic analysis of compressional structure in an active collision zone: the deformation of the Pinanshan Conglomerates, eastern Taiwan, *Proc. Geol. Soc. China*, *25*, 123-138.

Biq, C. (1971), Comparison of mélange tectonics in Taiwan and in some other mountain belts, *Pet. Geol. Taiwan*, *9*, 79-106.

Blisniuk, P. M., B. R. Hacker, J. Glodny, L. Ratschbacher, S. Bi, Z. Wu, M. O. McWilliams, and A. Calvert (2001), Normal faulting in central Tibet since at least 13.5 Myr ago, *Nature*, *412*, 628-632.

Chang, C. P., J. Angelier, C. Y. Huang, and C. S. Liu (2001), Structural evolution and significance of a mélange in a collision belt: the Lichi Mélange and the Taiwan arc-continent collision, *Geol. Mag.*, *138*, 633-651.

Chen, H.-H., and R.-J. Rau (2002), Earthquake locations and style of faulting in an active arc-continent plate boundary: the Chihshang fault of eastern Taiwan, *EOS, Trans., Am. Geophys. Uni.*, *83*(47), Fall Meet. Suppl., Abstract T61B-1277.

Chen, Y.-G. (1988), C-14 dating and correlation of river terraces along the lower reach of the Tahan-chi, northern Taiwan (in Chinese), M.S. thesis, 88pp., Natl. Taiwan Univ., Taipei.

Chu, H.-T., and M.-S. Yu (1997), *The Relationships between Earthquakes and Faults in the Taitung Longitudinal Valley* (in Chinese), Natl. Sci. Council Project Rep., Project No. NSC-86-2116-M-047-002, 133pp., Taipei.

Ho, C. S. (1986), A synthesis of the geologic evolution of Taiwan, *Tectonophysics*, *125*, 1-16.

Ho, C. S. (1988), *An Introduction to the Geology of Taiwan, Explanatory Text of the Geologic Map of Taiwan*, 2nd ed., 192pp., Cent. Geol. Surv., Ministry Econ. Affairs, Taipei, Taiwan.

Hsü, K. J. (1988), Mélange and the mélange tectonics of Taiwan, *Proc. Geol. Soc. China*, *31*(2), 87-92.

Hsu, T. L. (1956), Geology of the Coastal Range, eastern Taiwan, *Bull. Geol. Surv. Taiwan*, *8*, 39-63.

Hsu, Y.-J., M. Simons, S.-B. Yu, L.-C. Kuo, and H.-Y. Chen (2003), A two-dimensional dislocation model for interseismic deformation of the Taiwan mountain belt, *Earth Planet. Sci. Lett.*, *211*, 287-294.

Hu, J.-C., J. Angelier, C. Homberg, J.-C. Lee, and H.-T. Chu (2001), Three-dimensional modeling of the behavior of the oblique convergent boundary of southeast Taiwan: friction and strain partitioning, *Tectonophysics*, *333*, 261-276.

Huang, C.-Y., C.-T. Shyu, S. B. Lin, T.-Q. Lee, and D. D. Sheu (1992), Marine geology in the arc-continent collision zone off southeastern Taiwan: Implications for Late Neogene evolution of the Coastal Range, *Mar. Geol.*, *107*, 183-212.

Huang, C.-Y., W.-Y. Wu, C.-P. Chang, S. Tsao, P. B. Yuan, C.-W. Lin, and K.-Y. Xia (1997), Tectonic evolution of accretionary prism in the arc-continent collision terrane of Taiwan, *Tectonophysics*, *281*, 31-51.

Kuochen, H., Y.-M. Wu, C.-H. Chang, J.-C. Hu, and W.-S. Chen (2004), Relocation of the eastern Taiwan earthquakes and its tectonic implications, *Terr. Atmos. Oceanic Sci.*, *15*, 647-666.

Lallemand, S., and C.-S. Liu (1998), Geodynamic implications of present-day kinematics in the southern Ryukyus, *J. Geol. Soc. China*, *41*, 551-564.

Lee, J.-C., J. Angelier, H.-T. Chu, S.-B. Yu, and J.-C. Hu (1998), Plate-boundary strain partitioning along the sinistral collision suture of the Philippine and Eurasian plates: Analysis of geodetic data and geological observation in southeastern Taiwan, *Tectonics*, *17*, 859-871.

Lee, J.-C., J. Angelier, H.-T. Chu, J.-C. Hu, and F.-S. Jeng (2001), Continuous monitoring of an active fault in a plate suture zone: a creepmeter study of the Chihshang Fault, eastern Taiwan, *Tectonophysics*, *333*, 219-240.

Lee, J.-C., J. Angelier, H.-T. Chu, J.-C. Hu, F.-S. Jeng, and R.-J. Rau (2003), Active fault creep variations at Chihshang, Taiwan, revealed by creep meter monitoring, 1998-2001, *J. Geophys. Res.*, *108*(B11), 2528, doi:10.1029/2003JB002394.

Lin, C.-W., H.-C. Chang, S.-T. Lu, T.-S. Shih, and W.-J. Huang (2000), *An Introduction to the Active Faults of Taiwan, 2nd ed., Explanatory Text of the Active Fault Map of Taiwan* (in Chinese with English abstract), *Spec. Pub. Cent. Geol. Surv.*, *13*, 122pp., Taipei, Taiwan.

Malavieille, J., S. E. Lallemand, S. Dominguez, A. Deschamps, C.-Y. Lu, C.-S. Liu, P. Schnürle, and the ACT Scientific Crew (2002), Arc-continent collision in Taiwan: new marine observations and tectonic evolution, *Geol. Soc. Am. Spec. Paper*, *358*, 187-211.

Molnar, P., and P. Tapponnier (1978), Active tectonics of Tibet, *J. Geophys. Res.*, *83*, 5361-5375.

Oakeshott, G. B. (Ed.) (1975), *San Fernando, California Earthquake of 9 February 1971*, California Division of Mines and Geology Bulletin 196, 462pp., Sacramento, CA.

Page, B. M., and J. Suppe (1981), The Pliocene Lichi Mélange of Taiwan: its plate-tectonic and olistostromal origin, *Am. J. Sci.*, *281*, 193-227.

Sella, G. F., T. H. Dixon, and A. Mao (2002), REVEL: A model for Recent plate velocities from space geodesy, *J. Geophys. Res.*, *107*(B4), 2081, doi:10.1029/2000JB000033.

Shih, T.-T., J.-C. Chang, C.-E. Hwang, C.-D. Shih, G.-S. Yang, and Y.-M. Sunlin (1983), A geomorphological study of active fault in northern and eastern Taiwan (in Chinese with English abstract), *Geogr. Res.*, *9*, 20-72.

Shih, T.-T., J.-C. Chang, C.-E. Hwang, C.-D. Shih, and G.-S. Yang (1984), A geomorphological study of active fault in northern and eastern Taiwan, *Geogr. Studies*, *8*, 1-30.

Shih, T.-T., K.-H. Teng, J.-C. Chang, C.-D. Shih, and G.-S. Yang (1986), A geomorphological study of active fault in Taiwan (in Chinese with English abstract), *Geogr. Res.*, *12*, 1-44.

Shyu, J. B. H., K. Sieh, and Y.-G. Chen (2005a), Tandem suturing and disarticulation of the Taiwan orogen revealed by its neotectonic elements, *Earth Planet. Sci. Lett.*, *233*, 167-177.

Shyu, J. B. H., K. Sieh, Y.-G. Chen, and C.-S. Liu (2005b), Neotectonic architecture of Taiwan and its implications for future large earthquakes, *J. Geophys. Res.*, *110*, B08402, doi:10.1029/2004JB003251.

Shyu, J. B. H., K. Sieh, J.-P. Avouac, W.-S. Chen, and Y.-G. Chen (2006a) Millennial slip rate of the Longitudinal Valley fault from river terraces: Implications for convergence across the active suture of eastern Taiwan, *J. Geophys. Res.*, *111*, B08403, doi:10.1029/2005JB003971.

Shyu, J. B. H., K. Sieh, Y.-G. Chen, and L.-H. Chung (2006b) Geomorphic analysis of the Central Range fault, the second major active structure of the Longitudinal Valley suture, eastern Taiwan, *Geol. Soc. Am. Bull.*, *118*, 1447-1462.

Stuiver, M., and P. J. Reimer (1993), Extended ^{14}C data base and revised CALIB 3.0 ^{14}C age calibration program, *Radiocarbon*, *35*, 215-230.

Suppe, J. (1987), The active Taiwan mountain belt, in *Anatomy of Mountain Chains*, edited by J. P. Schaer, and J. Rodgers, pp. 277-293, Princeton Univ. Press, Princeton, N.J.

Teng, L. S. (1981), On the origin and tectonic significance of the Lichi Formation, Coastal Range, eastern Taiwan (in Chinese with English abstract), *Ti-Chih*, *3*, 51-61.

Teng, L. S. (1987), Stratigraphic records of the late Cenozoic Penglai orogeny of Taiwan, *Acta Geol. Taiwan.*, *25*, 205-224.

Teng, L. S. (1990), Late Cenozoic arc-continent collision in Taiwan, *Tectonophysics*, *183*, 57-76.

Teng, L. S., and Y. Wang (1981), Island arc system of the Coastal Range, eastern Taiwan, *Proc. Geol. Soc. China*, *24*, 99-112.

Wang, Y., and W.-S. Chen (1993), Geologic Map of Eastern Coastal Range, Central Geological Survey, MOEA, scale 1:100,000, Taipei.

Wu, Y. M., Y. G. Chen, T. C. Shin, H. Kuochen, C. S. Hou, J. C. Hu, C. H. Chang, C. F. Wu, and T. L. Teng (2006), Coseismic versus interseismic ground deformations, fault rupture inversion and segmentation revealed by 2003 Mw 6.8 Chengkung earthquake in eastern Taiwan, *Geophys. Res. Lett.*, *33*, L02312, doi:10.1029/2005GL024711.

Yang, G.-S. (1986), A geomorphological study of active faults in Taiwan – especially on the relation between active faults and geomorphic surfaces (in Chinese), Ph.D. thesis, 178pp., Chinese Culture Univ., Taipei, Taiwan.

Yin, A., P. A. Kapp, M. A. Murphy, C. E. Manning, T. M. Harrison, M. Grove, L. Ding, X.-G. Deng, and C.-M. Wu (1999), Significant late Neogene east-west extension in northern Tibet, *Geology*, *27*, 787-790.

Yu, S.-B., and L.-C. Kuo (2001), Present-day crustal motion along the Longitudinal Valley Fault, eastern Taiwan, *Tectonophysics*, *333*, 199-217.

Yu, S.-B., and C.-C. Liu (1989), Fault creep on the central segment of the Longitudinal Valley fault, eastern Taiwan, *Proc. Geol. Soc. China*, *32*, 209-231.

Yu, S.-B., G.-K. Yu, L.-C. Kuo, and C. Lee (1992), Crustal deformation in the southern Longitudinal Valley area, eastern Taiwan, *J. Geol. Soc. China*, *35*, 219-230.

Figure captions

Figure 1. The island of Taiwan is being created by a tandem suturing of the Luzon volcanic arc and a sliver of continental crust to the Chinese continental margin. The Longitudinal Valley suture (LVS) is the eastern of the two sutures. It joins the Coastal Range (CoR), the docked part of the Luzon volcanic arc, and the continental sliver of the Central Range (CeR), the mountainous backbone of the island. Current velocity vectors of the Philippine Sea plate relative to South China, at 124°E and 20°, 21°, and 22°N, are calculated using the Recent plate velocity model (REVEL) of *Sella et al.* [2002]. Current velocity vector of the Ryukyu arc is adapted from *Lallemand and Liu* [1998]. Black dashed lines are the northern and western limits of the Wadati-Benioff zone of the two subduction zones, taken from the seismicity database of the Central Weather Bureau, Taiwan. DF: deformation front; LCS: Lishan-Chaochou suture; WF: Western Foothills; HP: Hengchun Peninsula. This figure is adapted from *Shyu et al.* [2005a].

Figure 2. Map of neotectonic domains of southeastern Taiwan, modified from *Shyu et al.* [2005b]. Each domain contains a distinct assemblage of active structures. Two domains, the Hualien and Taitung Domains, are present in eastern Taiwan along the Longitudinal Valley suture. LVF: Longitudinal Valley fault; CRF: Central Range fault. Bold light green and pink lines are boundaries of domains.

Figure 3. Major fluvial landforms near the southernmost Longitudinal Valley. Between the Central and Coastal Ranges are several uplifted fluvial surfaces. South of the Luyeh River, the Peinanshan is an elongate hill underlain by fluvial Peinanshan Conglomerate and capped by lateritic fluvial terraces. North of the Luyeh River, the Kaotai terraces are lateritized fluvial surfaces that may be correlative with the highest surfaces of the Peinanshan. East of the Luliao River, the lower Pingting terraces are

underlain by young, thin uplifted Peinan River gravels deposited on Lichi Formation.

Figure 4. Detailed map of geomorphic features and active structures of the Kaotai terraces area. Note that the names of terraces indicate only the relative ages of the terraces and do not imply correlation of the terraces; that is, terrace 4 north of the Luyeh River may not be the same age as terrace 4 elsewhere. The Luyeh strand, a major strand of the Longitudinal Valley fault, runs along the western edge of the Kaotai terraces and has produced a monoclinal scarp on the Lungtien terrace to the south. To the north, the Luyeh strand dies out just south of the Luliao River. The other strand of the Longitudinal Valley fault, the Peinan strand, runs within the Peinan River valley and through the Luanshan Bridge (LSB) about 200 m from the eastern end of the bridge. Ages of terraces are calibrated ages (2σ), in cal BP.

Figure 5. Selected topographic profiles of the Kaotai terraces area. Locations of the profiles appear in Figure 4. (a) A topographic profile across the Lungtien and other terraces. The Luyeh strand produced a monoclinal scarp, about 15 m high, about halfway downstream on the Lungtien terrace (terrace 4). Other than the scarp, the terrace surface shows a gentle eastward slope that is consistent with the modern Luyeh River bed. Notice that at the downthrown (west) side of the Luyeh strand, the Lungtien terrace is still about 60 m above the current Luyeh River bed. We hypothesize that the Longitudinal Valley and eastern flank of the Central Range are on the hanging-wall block of a deeper Central Range fault that dips west, under the Central Range. (b) A short topographic profile across the Luyeh strand on terrace 3. The terrace east of the Luyeh strand is about 10 m higher than its counterpart west of the strand.

Figure 6. Field photographs of several deformed bridges across the Peinan River. (a) About 200 m from its eastern end, the Luanshan Bridge has been fractured, with its

eastern part displaced relatively westward. View is toward the south. (b) Near the eastern end of the Lichi Bridge, an eastern section of the bridge appears to have moved upward and caused deformation of its contact with its neighboring section to the west. The lower part of the contact appears to have opened and the upper part of the contact appears to have narrowed. View is toward the north. (c) About 100 m from its eastern end, the Paohua Bridge has been deformed by the Longitudinal Valley fault. The eastern part of the bridge has moved upward with respect to its western part. View is toward the west.

Figure 7. Detailed map of geomorphic features and active structures of the northern Peinanshan area. The Luyeh strand runs along the western front of the Peinanshan. An anticline and a syncline in the hanging-wall block of the Luyeh strand clearly deform the highest terrace 7 atop the northern Peinanshan. The Peinan strand cuts through the northeastern corner of the Peinanshan and may be predominantly left-lateral. An immense landslide deposit covers a fluvial strath, about 80 m above the modern Peinan River bed, east of the Peinan River on the western flank of the Coastal Range. Brown lines indicate head scarps of blocks, sometimes within the landslide complex. Ages of wood fragments found in the landslide deposits are calibrated ages (2σ), in cal BP.

Figure 8. Selected topographic profiles of the northern Peinanshan area. Locations of the profiles appear in Figure 7. (a) A topographic profile of terrace 7 atop the northern Peinanshan. The fluvial surface has been deformed into an asymmetrical syncline in the east and an anticline in the west. (b) The topographic profile of lower terraces on the south side of the Luyeh River north of terrace 7 indicates that these lower terraces are also deformed by the folds, but to a lesser degree. This suggests that the folds have been growing during incision of the Luyeh River.

Figure 9. Photographs of the landslide deposits on the eastern bank of the Peinan River. (a) The landslide sits on a fluvial strath, now about 80 m above the modern Peinan River bed, on rocks of the Lichi Formation and the Peinanshan Conglomerate. The location from which the photo was taken and its view direction are shown in Figure 7. (b) A thin layer of rounded fluvial gravels, about 1-2 m thick, lies between the strath and the landslide deposits. The photo was taken at point G in Figure 7, looking to the north. (c) The contact between the Lichi Formation and the Peinanshan Conglomerate, which may be an old fault, is covered by the fluvial gravels and the landslide deposits. No offset along this contact is present in the fluvial gravels or the landslide deposits. The photo was taken in a small westward flowing canyon, at point K in Figure 7, looking to the south.

Figure 10. Detailed map of geomorphic features and active structures of the southern Peinanshan area. The Luyeh strand runs along the western front of the Peinanshan, but becomes an E-W striking monocline that wraps around the southernmost part of the Peinanshan. The Peinan strand traverses the Peinan River valley, but produces a small N-S scarp on the terraces near Lichi.

Figure 11. Detailed map of geomorphic features and active structures of the Pingting terraces area. The Luyeh strand steps to the east and joins with the Peinan strand to form the main strand of the Longitudinal Valley fault. The fault has several minor strands, along the western flank of the Pingting terraces. The eastern strand clearly shows sinistral as well as reverse offset. The age of the terraces are shown in calibrated ages (2σ), in cal BP.

Figure 12. A schematic tectonic E-W cross section at the latitude of the Peinanshan shows the proposed tectonic model for the southern end of the Taitung Domain. The

east-dipping Longitudinal Valley fault (LVF) branches into the Luyeh strand (LS) and the Peinan strand (PS), between which late Quaternary fluvial surfaces and the Peinanshan Conglomerate (PNS) are progressively deformed. The Luyeh strand crops out along the western edge of the Peinanshan, while the Peinan strand traverses the Peinan River valley. The west-dipping Central Range fault appears to be blind in this area and is overridden by the Longitudinal Valley fault. However, the uplifted and deformed terraces along the upper reach of the Luyeh River suggest the Central Range fault is also active.

Figure 13. Schematic crustal cross-sections show our hypothesis of the "Christmas tree" model for the evolution of the Longitudinal Valley suture, from *Shyu et al.* [2006b]. Each section is drawn using current topography and observations along the lines specified on the index map, with no vertical exaggeration. Red indicates the youngest and currently active faults in each time frame, and blue indicates older faults, which may still be active. Faults are dashed where inferred. (a) Before suturing, the Luzon forearc oceanic lithosphere (FAO) subducts beneath the Central Range continental sliver (CR). (b) As the Luzon volcanic arc lithosphere (LVA) approaches the Central Range, an east-dipping thrust fault appears, allowing the FAO to also subduct underneath the LVA. Contemporaneously on the west side of the valley, the proximity of the LVA to the CR induces formation of a newer, shallower west-dipping thrust fault above the original one. This is the current structural geometry near the southern end of the Longitudinal Valley, the area of analysis of this study. (c) As the suture matures, the two non-oceanic lithospheric blocks both start to thicken by evolving multiple reverse-fault wedges, with the younger ones at shallower depth. (d) At the latitude of about 23°30'N, the suture is nearing maturity. The suture has evolved into a "Christmas tree" shape, with a thick pile of sediments between the two non-oceanic lithospheric blocks and underlain by the subducted forearc oceanic lithosphere. (e) In northern Longitudinal Valley, the dominantly sinistral Longitudinal Valley fault appears to be the only major active

structure. The west-dipping Central Range fault has become inactive, and sediments in the Longitudinal Valley are lapping on the eastern flank of the Central Range. Relocated earthquake hypocenters in (c) and (d) are adapted from Kuochen et al. (2004).

Table 1. List and analytical results of the charcoal samples dated in this research.

Table 1

Sample number	Site name	GPS location of site		Corresponding figure	Terrace level	Age (yrBP)	Calibrated age (2σ)(cal BP)#
		X	Y				
BN-02B	BN	258439	2534148	4	4	3130±30*	3260-3440
20010917-2	CYB	264514	2533951	4	2	1170±80*	940-1260
LS-01 LS-02 LS-03	LSB	265256	2532808	7	++	2310±80^ 2250±70^ 850±60^	2120-2710 2040-2360 670-910
RY2-05	RY2	266018	2538348	11	4	1700±30*	1530-1690

Calibrated using the CALIB program [*Stuiver and Reimer*, 1993].

* These samples were dated in Lawrence Livermore National Laboratory using AMS.

^ These samples were dated in National Taiwan University by conventional ^{14}C dating.

++ Landslide complex.

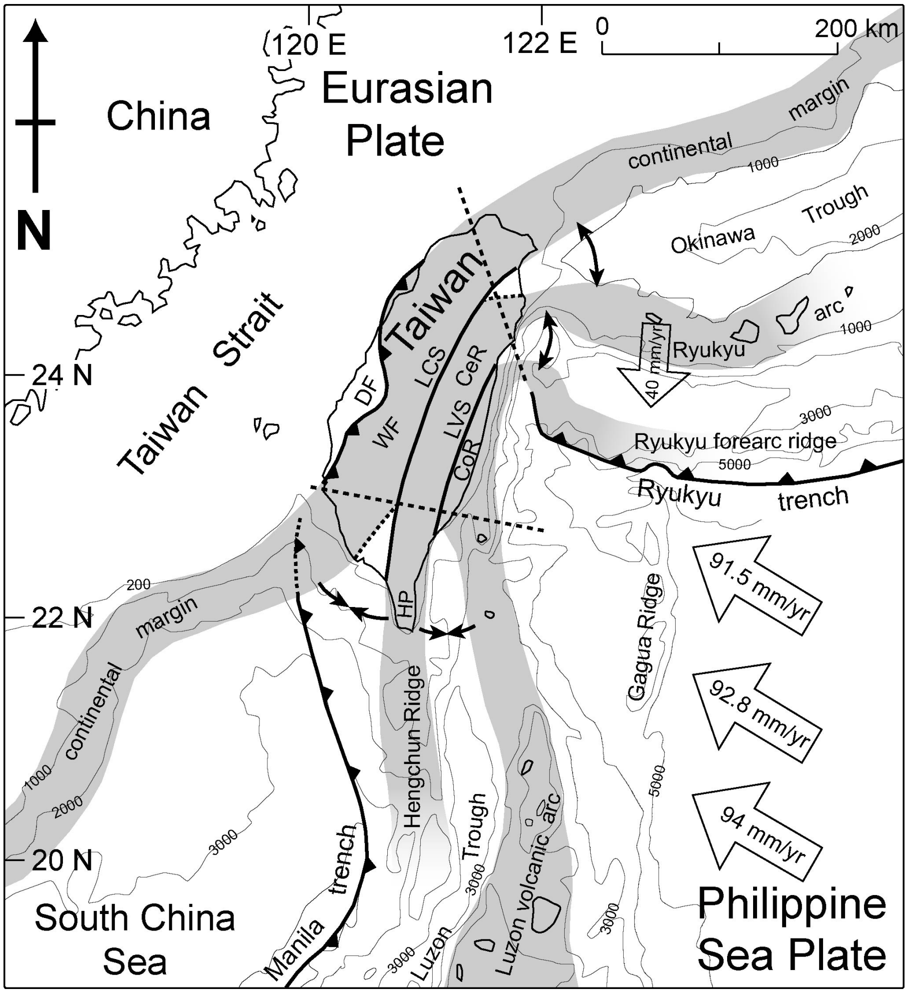
N
120 E
122 E
0
200 km
China
Eurasian Plate
continental margin
1000
Okinawa
Trough
2000
arc
Ryukyu
40 mm/yr
Taiwan
Taiwan Strait
24 N
DF
WF
LCS
CeR
LVS
CoR
3000
Ryukyu forearc ridge
5000
Ryukyu trench
91.5 mm/yr
200
22 N
margin
HP
Gagua Ridge
continental
92.8 mm/yr
Hengchun Ridge
1000
2000
5000
94 mm/yr
Trough
Luzon volcanic arc
3000
20 N
trench
South China Sea
Manila
Luzon
Philippine Sea Plate

Figure 1

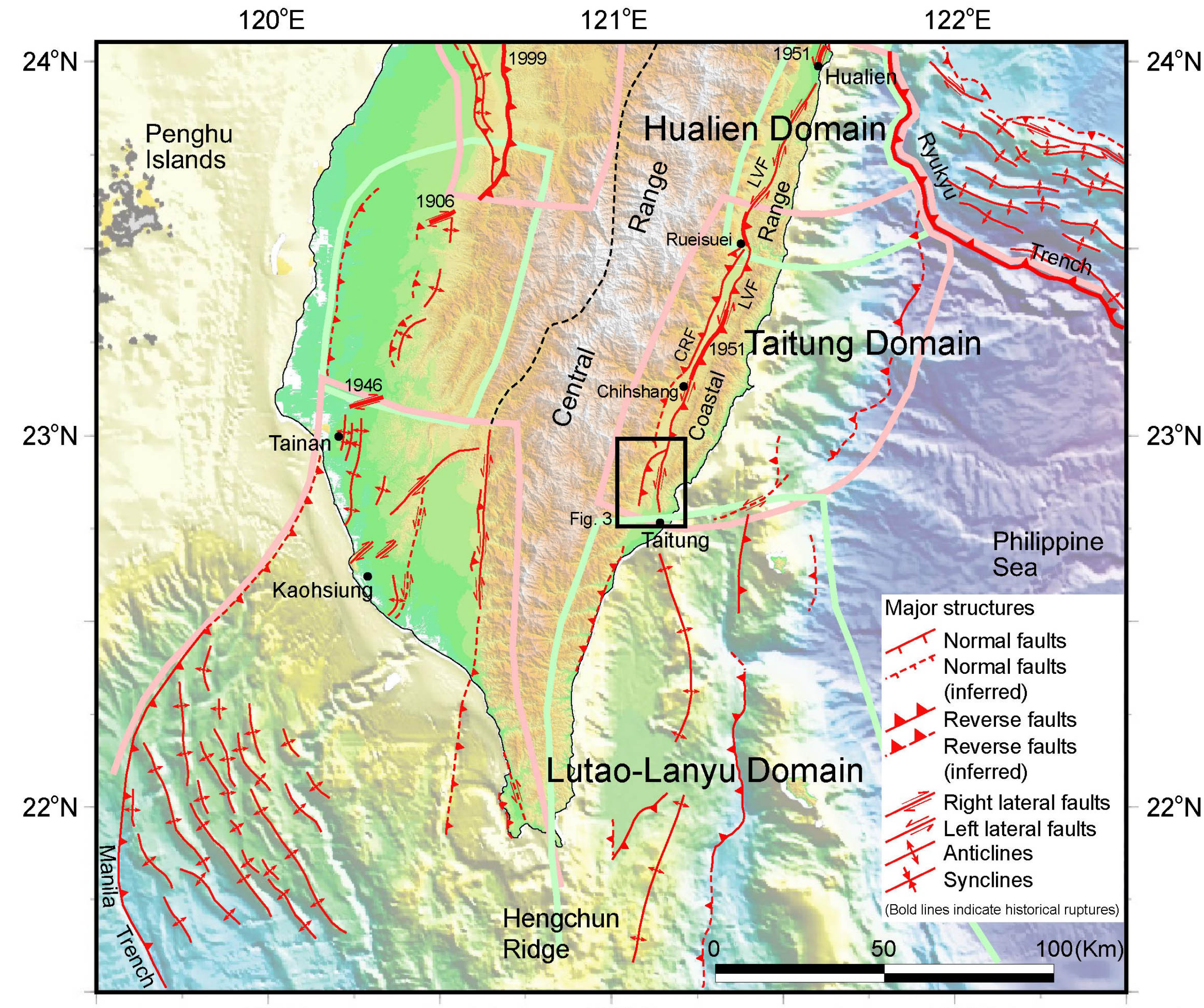

120°E
121°E
122°E
24°N
23°N
22°N
Penghu Islands
1999
1951
Hualien
Hualien Domain
Ryukyu
Trench
1906
Central
Range
Rueisuei
LVF
Range
CRF
1951
Taitung Domain
1946
Chihshang
Coastal
Tainan
Fig. 3
Taitung
Kaohsiung
Philippine Sea
Major structures
Normal faults
Normal faults (inferred)
Reverse faults
Reverse faults (inferred)
Right lateral faults
Left lateral faults
Anticlines
Synclines
(Bold lines indicate historical ruptures)
Lutao-Lanyu Domain
Manila Trench
Hengchun Ridge
0
50
100(Km)

Figure 2

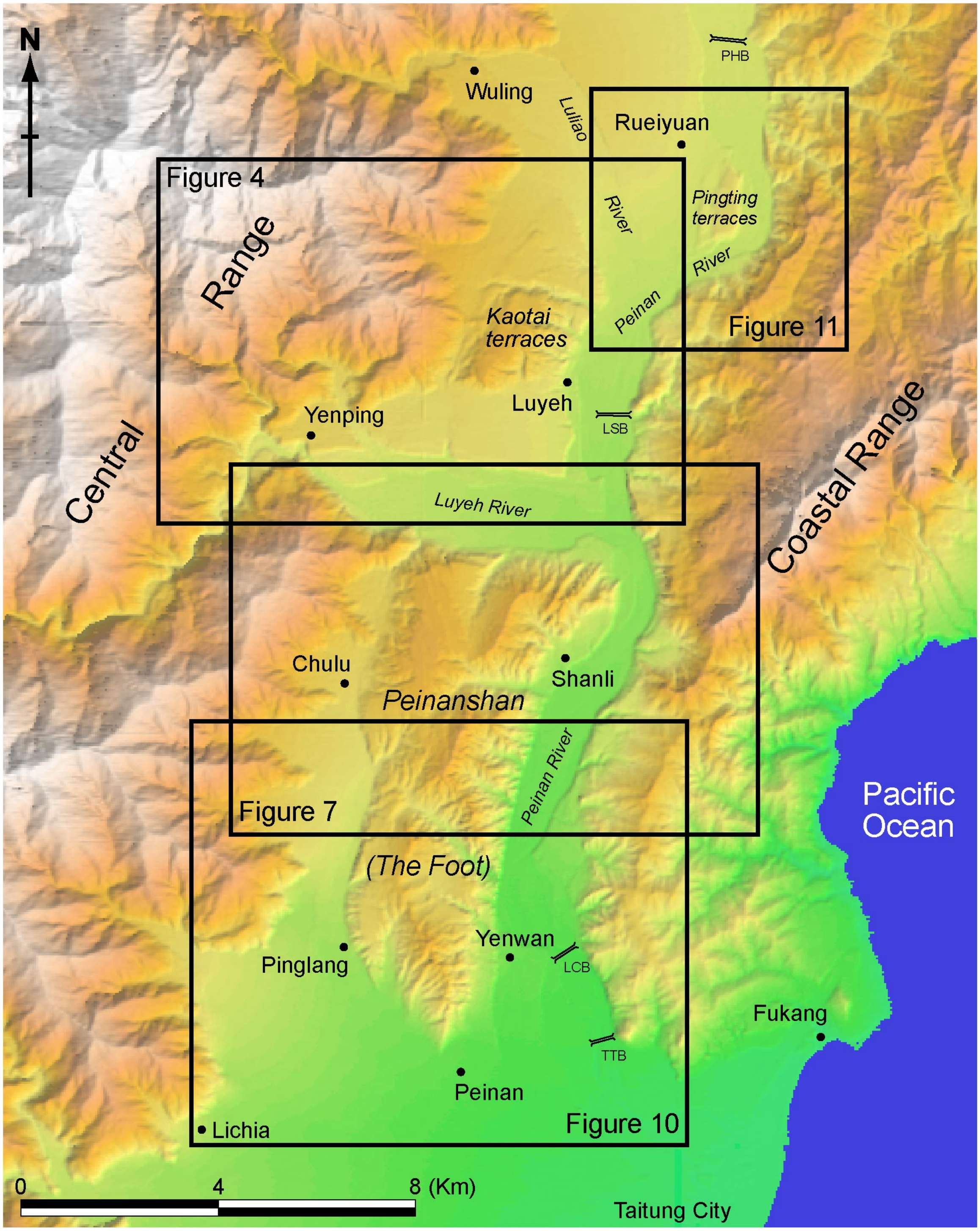

N
PHB
Wuling
Luliao
Rueiyuan
Figure 4
River
Pingting terraces
Range
River
Peinan
Kaotai terraces
Figure 11
Luyeh
Yenping
LSB
Central
Coastal Range
Luyeh River
Chulu
Shanli
Peinanshan
Peinan River
Pacific Ocean
Figure 7
(The Foot)
Yenwan
Pinglang
LCB
Fukang
TTB
Peinan
Lichia
Figure 10
0
4
8 (Km)
Taitung City

Figure 3

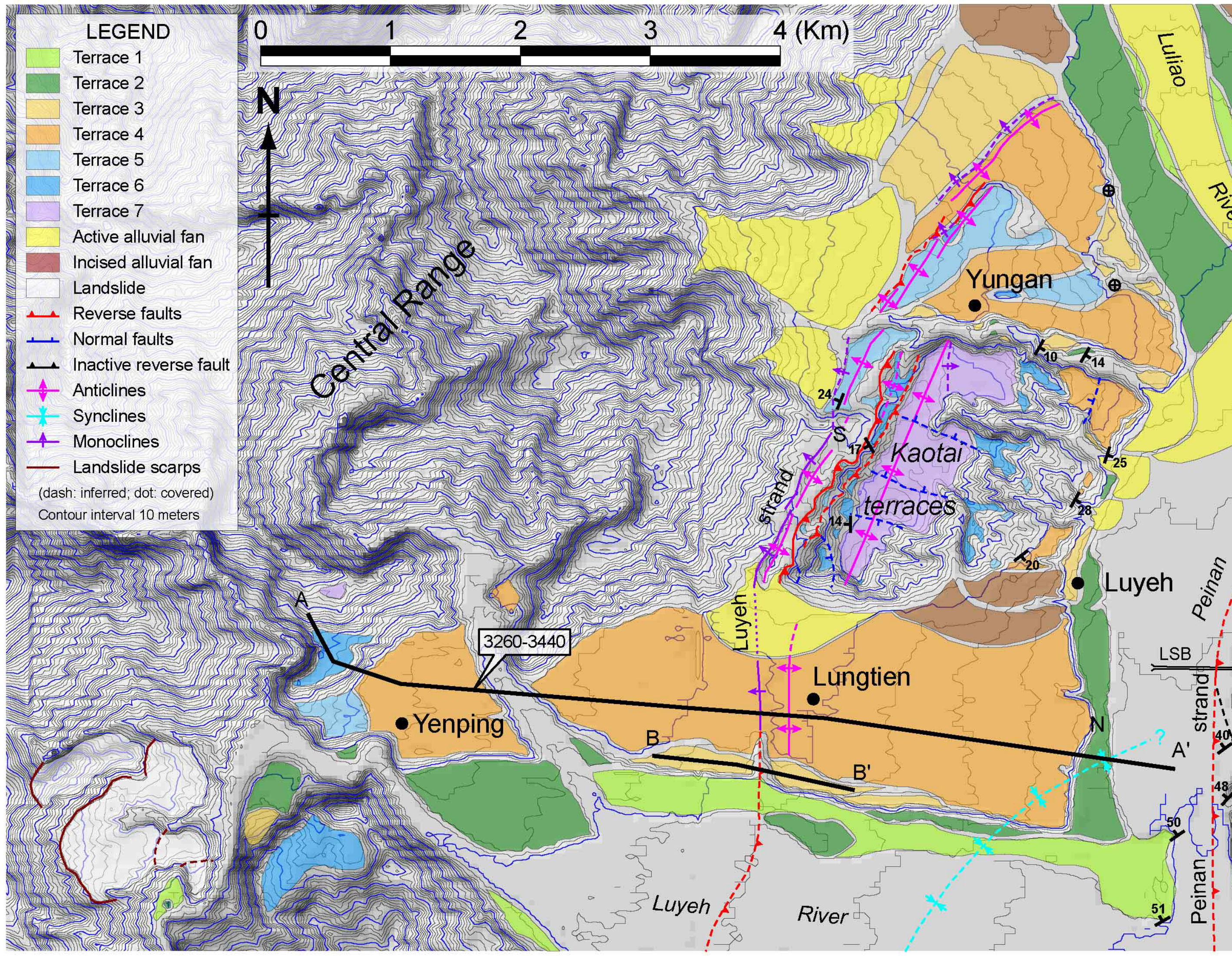
LEGEND
Terrace 1
Terrace 2
Terrace 3
Terrace 4
Terrace 5
Terrace 6
Terrace 7
Active alluvial fan
Incised alluvial fan
Landslide
Reverse faults
Normal faults
Inactive reverse fault
Anticlines
Synclines
Monoclines
Landslide scarps
(dash: inferred; dot: covered)
Contour interval 10 meters
0
1
2
3
4 (Km)
N
Central Range
Luliao
Yungan
Kaotai
terraces
strand
Luyeh
Lungtien
Yenping
3260-3440
A
A'
B
B'
LSB
Peinan
Luyeh
River

Figure 4

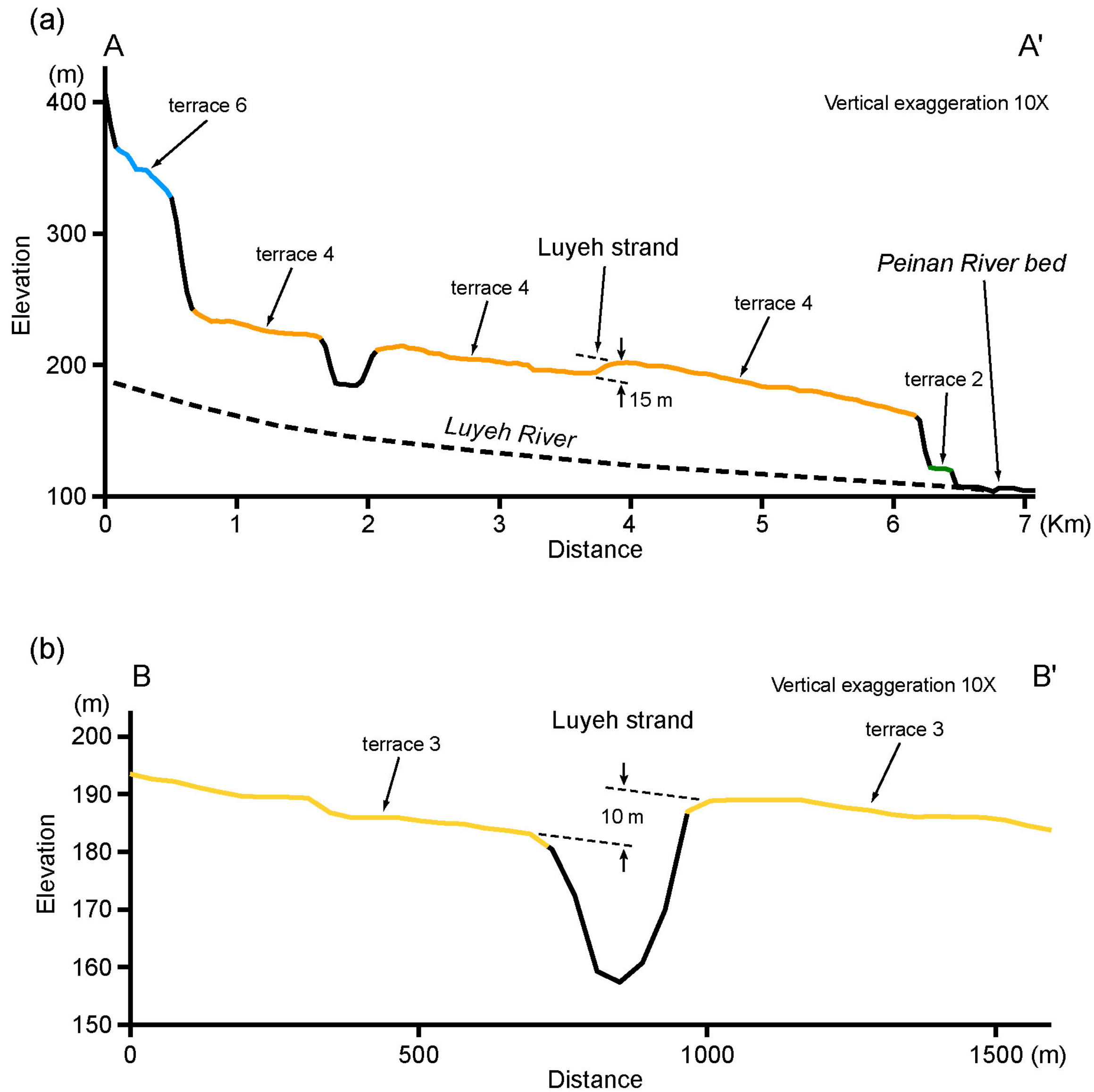
(a)
A
A'
(m)
400
300
200
100
Vertical exaggeration 10X
terrace 6
terrace 4
terrace 4
Luyeh strand
terrace 4
Peinan River bed
terrace 2
15 m
Luyeh River
Elevation
0
1
2
3
4
5
6
7 (Km)
Distance
(b)
B
B'
Vertical exaggeration 10X
(m)
200
190
180
170
160
150
Luyeh strand
terrace 3
terrace 3
10 m
Elevation
0
500
1000
1500 (m)
Distance

Figure 5

Figure 6

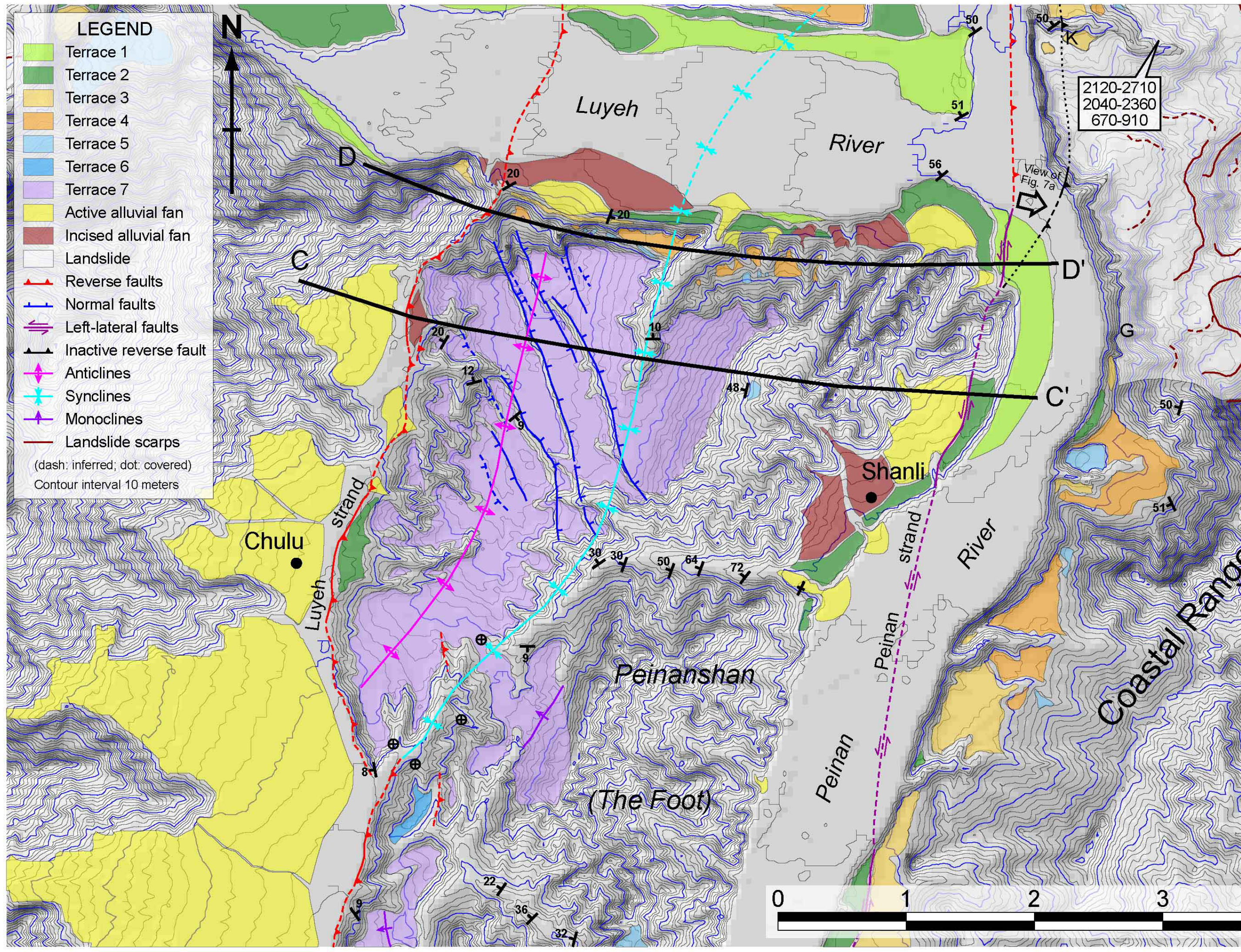
LEGEND
Terrace 1
Terrace 2
Terrace 3
Terrace 4
Terrace 5
Terrace 6
Terrace 7
Active alluvial fan
Incised alluvial fan
Landslide
Reverse faults
Normal faults
Left-lateral faults
Inactive reverse fault
Anticlines
Synclines
Monoclines
Landslide scarps
(dash: inferred; dot: covered)
Contour interval 10 meters
N
Luyeh
River
D
D'
C
C'
Chulu
Luyeh
strand
Shanli
Peinanshan
(The Foot)
Peinan
strand
River
Peinan
Coastal Range
2120-2710
2040-2360
670-910
0
1
2
3

Figure 7

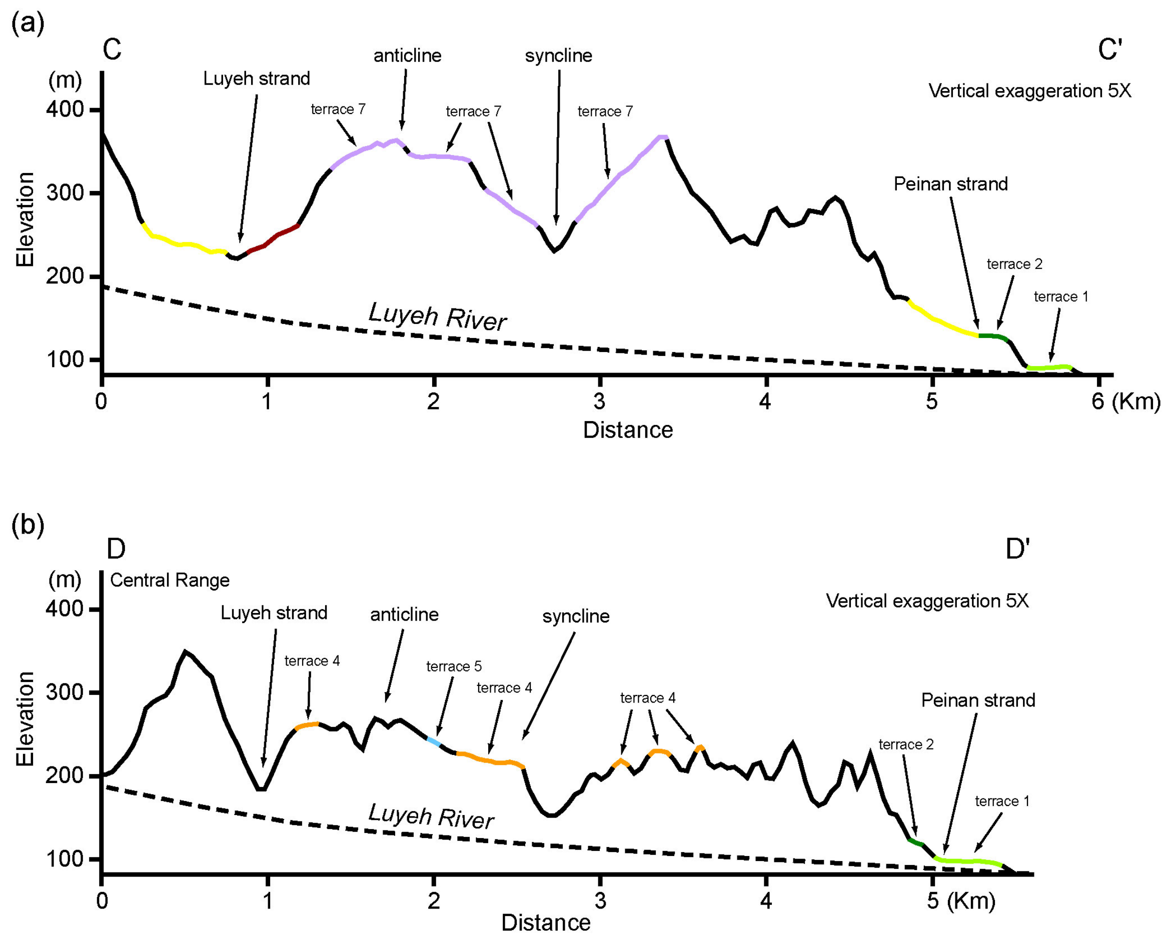
(a)
C
C'
(m)
400
300
200
100
Elevation
Luyeh strand
terrace 7
anticline
terrace 7
syncline
terrace 7
Vertical exaggeration 5X
Peinan strand
terrace 2
terrace 1
Luyeh River
0
1
2
3
4
5
6 (Km)
Distance
(b)
D
D'
(m)
Central Range
400
300
200
100
Elevation
Luyeh strand
terrace 4
anticline
terrace 5
terrace 4
syncline
terrace 4
Vertical exaggeration 5X
Peinan strand
terrace 2
terrace 1
Luyeh River
0
1
2
3
4
5 (Km)
Distance

Figure 8

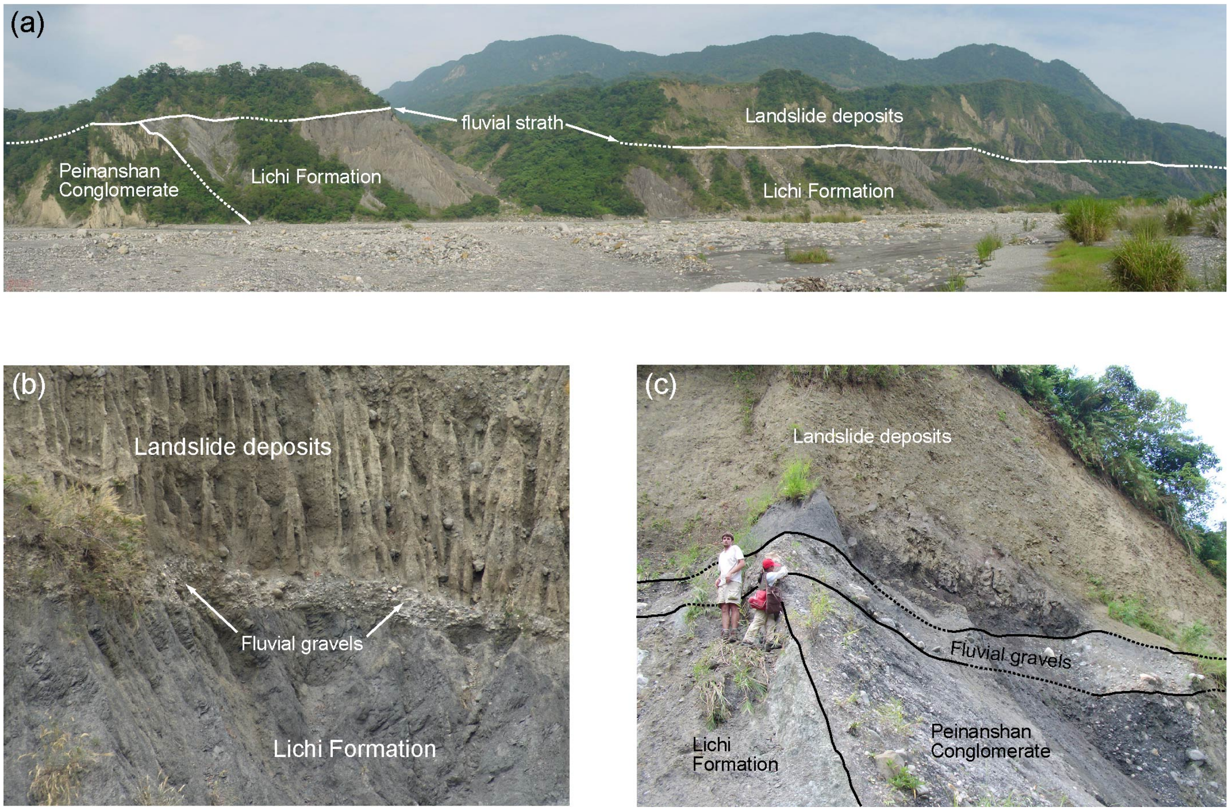
(a)
fluvial strath
Landslide deposits
Peinanshan
Conglomerate
Lichi Formation
Lichi Formation
(b)
Landslide deposits
Fluvial gravels
Lichi Formation
(c)
Landslide deposits
Fluvial gravels
Lichi
Formation
Peinanshan
Conglomerate

Figure 9

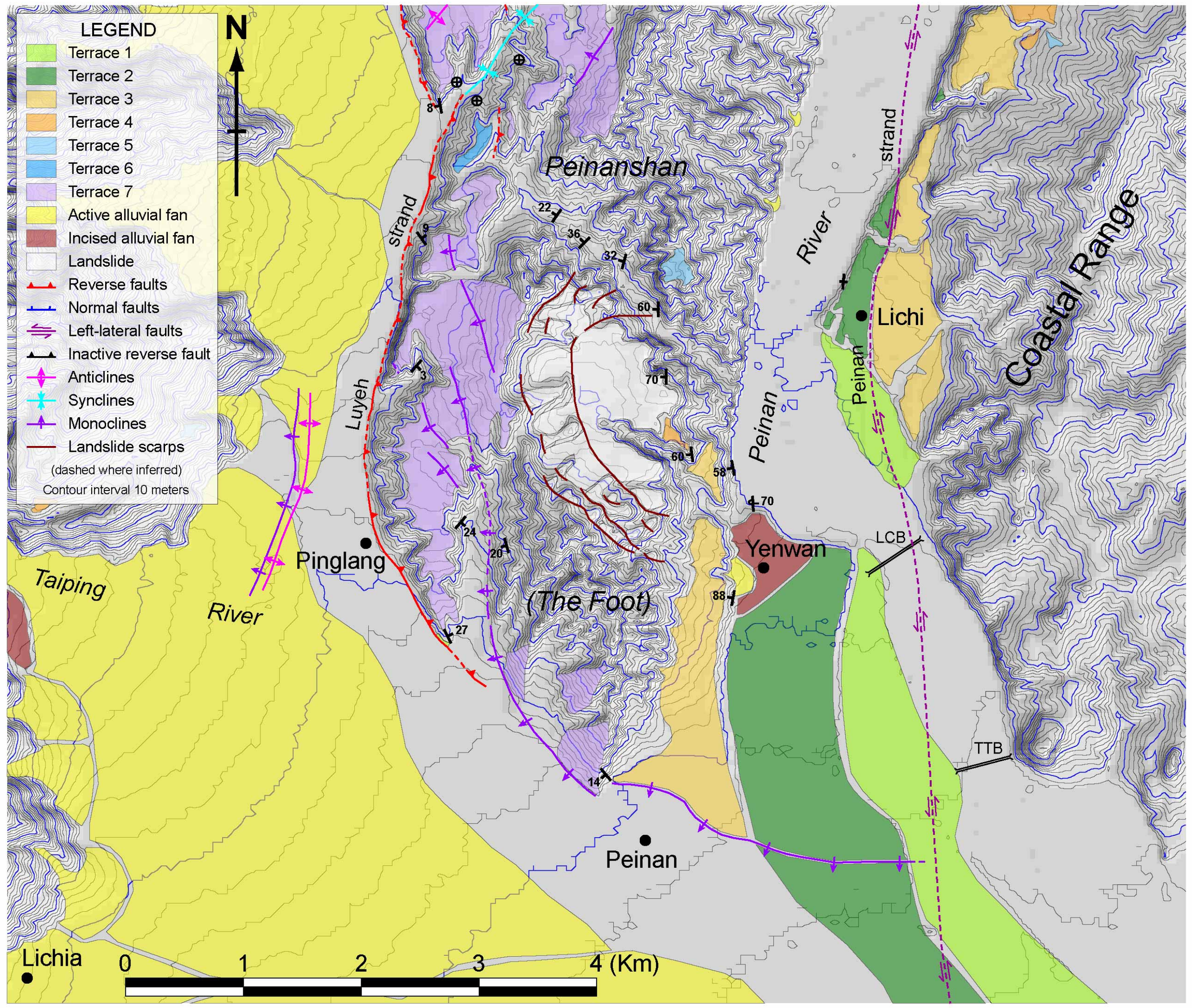

LEGEND
Terrace 1
Terrace 2
Terrace 3
Terrace 4
Terrace 5
Terrace 6
Terrace 7
Active alluvial fan
Incised alluvial fan
Landslide
Reverse faults
Normal faults
Left-lateral faults
Inactive reverse fault
Anticlines
Synclines
Monoclines
Landslide scarps
(dashed where inferred)
Contour interval 10 meters
N
Peinanshan
strand
Luyeh
strand
River
Peinan
River
Peinan
Lichi
Coastal Range
Pinglang
Taiping
River
(The Foot)
Yenwan
LCB
TTB
Peinan
Lichia
0
1
2
3
4 (Km)

Figure 10

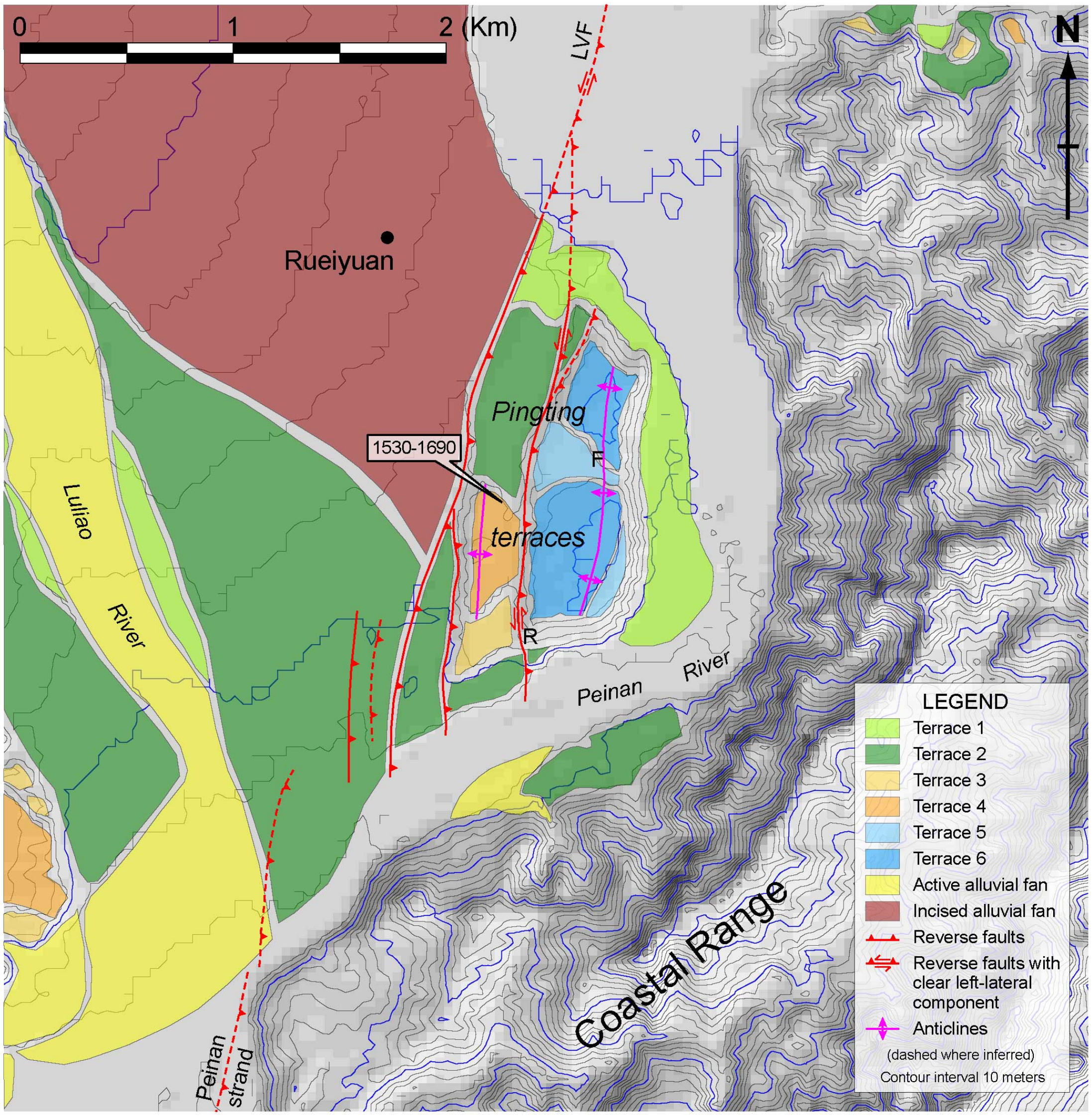
0
1
2 (Km)
LVF
N
Rueiyuan
Pingting
1530-1690
F
terraces
R
Luliao
River
Peinan
River
Coastal Range
Peinan
strand
LEGEND
Terrace 1
Terrace 2
Terrace 3
Terrace 4
Terrace 5
Terrace 6
Active alluvial fan
Incised alluvial fan
Reverse faults
Reverse faults with clear left-lateral component
Anticlines
(dashed where inferred)
Contour interval 10 meters

Figure 11

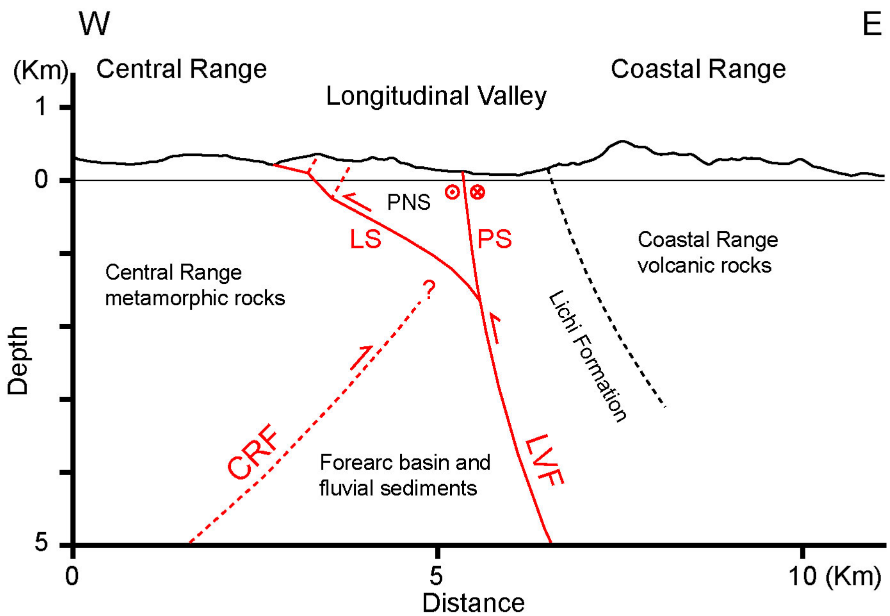
W
E
(Km)
Central Range
Longitudinal Valley
Coastal Range
1
0
PNS
LS
PS
Coastal Range
volcanic rocks
Central Range
metamorphic rocks
?
Lichi Formation
Depth
CRF
Forearc basin and
fluvial sediments
LVF
5
0
5
10 (Km)
Distance

Figure 12

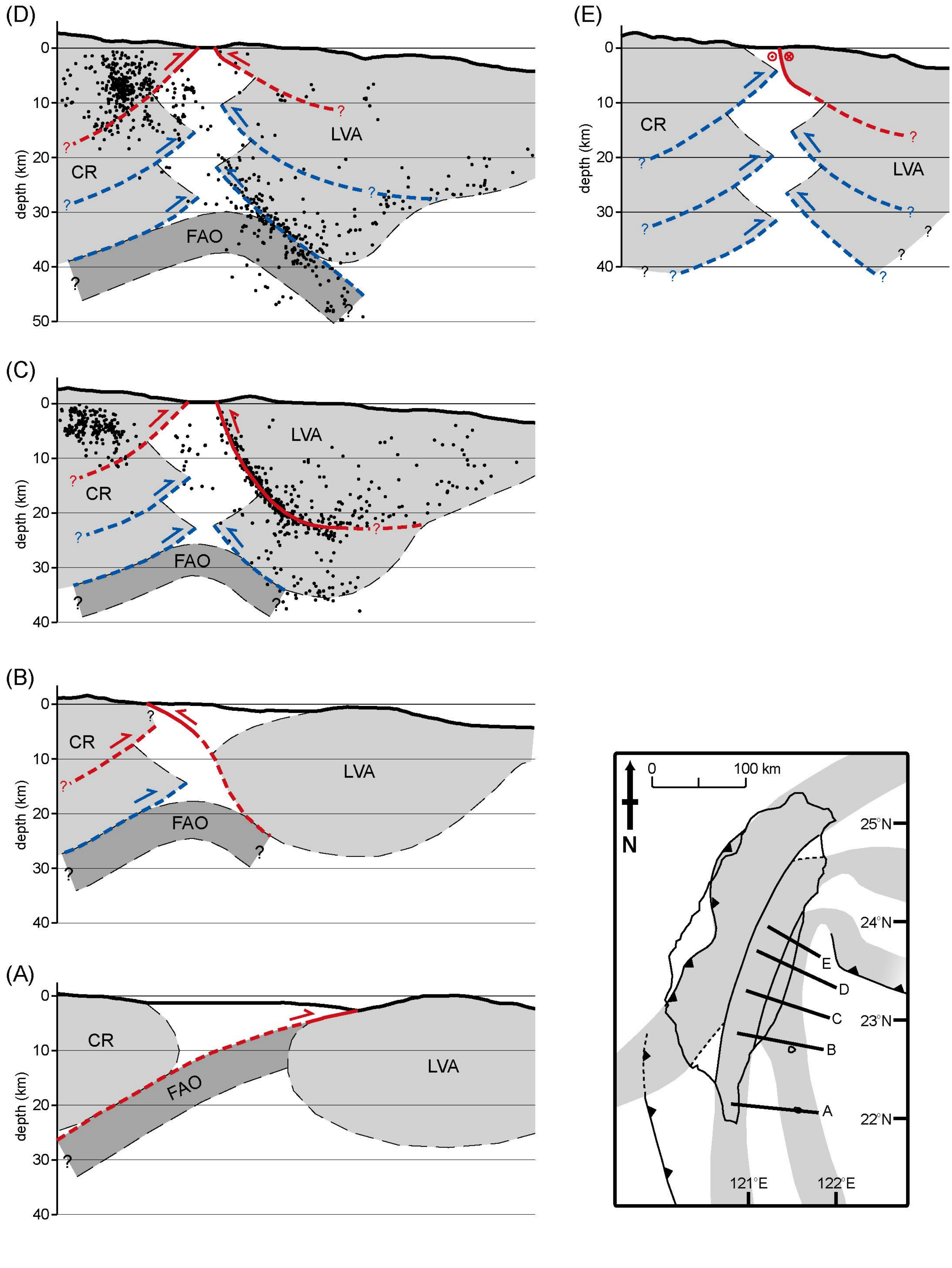

(D)
(E)
(C)
(B)
(A)
depth (km)
CR
LVA
FAO
0
10
20
30
40
50
?
0
100 km
N
25°N
24°N
23°N
22°N
121°E
122°E
A
B
C
D
E

Figure 13